ACIBADEM MEHMET ALI AYDINLAR UNIVERSITY
INSTITUTE OF HEALTH SCIENCES

THE EFFECT OF HIGH DENSITY LIPOPROTEIN (HDL) ON AUTOPHAGY AND MITOCHONDRIAL DYNAMICS IN A MONOCYTIC CELL LINE

SİMGE ŞENAY

M.Sc. THESIS

DEPARTMENT OF MEDICAL BIOTECHNOLOGY

SUPERVISOR
Assoc. Prof. Devrim Öz Arslan

ISTANBUL-2022

ACIBADEM MEHMET ALI AYDINLAR UNIVERSITY
INSTITUTE OF HEALTH SCIENCES

THE EFFECT OF HIGH DENSITY LIPOPROTEIN (HDL) ON AUTOPHAGY AND MITOCHONDRIAL DYNAMICS IN A MONOCYTIC CELL LINE

SİMGE ŞENAY

M.Sc. THESIS

DEPARTMENT OF MEDICAL BIOTECHNOLOGY

SUPERVISOR
Assoc. Prof. Devrim Öz Arslan

ISTANBUL-2022

DECLARATION

I declare that this thesis work is my own work, I had no unethical behavior at any stages from the planning to the writing of the thesis, I obtained all the information in this thesis in accordance with academic and ethical rules, I cited all the information and comments that were not obtained with this thesis work, and I provided resources in the list of references. I also declare that there was no violation of any patents and copyrights during the study and writing of this thesis.

06/07/2022
Simge Şenay

PREFACE AND ACKNOWLEDGEMENT

First and foremost, I would like to give my appreciation to my supervisor Assoc. Prof. Devrim Öz Arslan for her time, patience, guidance, and generously giving me the opportunity to learn in her laboratory. I would like to thank Asst. Prof. Deniz Ağırbaşlı for her time, help, advice, and contribution during this project. I am also thankful to Prof. Beki Kan for her teachings and suggestions during this thesis study.

My gratitude goes out to all my colleagues in our department; Demet Açıkgöz, Hande Kasap Can, Hande İpek Yetke, and Tuğçe Demir Özüpek who supported and helped me tremendously through this project.

I would like to sincerely thank Ayşegül Ekmekçioğlu, Merve Büşra Çatakçı, Dilan Acar, Nesteren Mansur Özen, Sümeyye Akçelik Deveci, İlayda Şahin, Ece Aksoy, Esma Aybakan, Gözde Ervin Köle, and Özgür Yılmaz for all their help whenever I needed and making the fifth floor a better place. My appreciation also goes to Görkem Gün and other members of the Acıbadem Mehmet Ali Aydınlar University Research Laboratory Center.

My biggest appreciation goes to my parents for their endless support and infinite faith in my studies since day one. I am also forever grateful for my dearest friends Tülay Aydın and İrem Akbulak, for their support and wise counsels. My sincere gratitude goes to Ülgen Sarıkavak and our cat Hulusi for always being there and helping me get through the bad times together.

I would also like to thank Acıbadem Mehmet Ali Aydınlar University for providing laboratory facilities and Scientific and Technological Research Council of Turkey (TUBITAK) for their financial support.

This study was supported by TUBITAK 3501 project (117S078) and Acıbadem Mehmet Ali Aydınlar University (ABAPKO 2020/03/10). I was supported as a fellow from 2018 to 2021.

TABLE OF CONTENTS

LIST OF ABBREVIATIONS

ABCA1	ATP Binding Cassette Transporter A1
ABCG1	ATP Binding Cassette Subfamily G Member 1
apoA-I	Apolipoprotein AI
apoA-II	Apolipoprotein AII
apoB	Apolipoprotein B
APS	Ammonium persulfate
ATCC	American Type Culture Collection
ATG	Autophagy-related
ATP	Adenosine triphosphate
ATP III	Adult Treatment Panel III
Bafilo	Bafilomycin
BECN1	Beclin-1
BSA	Bovine Serum Albumin
Ca^{2+}	Calcium
CAD	Coronary artery disease
CO_2	Carbon dioxide
DAPI	4′,6-diamidino-2-phenylindole
ddH_2O	Double distilled water
dH_2O	Distilled water
DMSO	Dimethyl sulfoxide
DNA	Deoxyribonucleic acid
dPBS	Dulbecco's phosphate-buffered saline
DTT	1,4-dithiothreitol
EDTA	Ethylenediaminetetraacedic acid
eNOS	Endothelial Nitric Oxide Synthase
ER	Endoplasmic Reticulum
ETC	Electron Transport Chain
FBS	Fetal Bovine Serum
FITC	Fluorescein isothiocyanate
FSC	Forward Scatter

h	Hours
HCl	Hydrochloric acid
HDL	High Density Lipoprotein
HDL-C	High Density Lipoprotein Cholesterol
IFN-γ	Interferon gamma
IgG	Immunoglobulin G
IL	Interleukin
KCl	Potassium chloride
KH_2PO_4	Potassium phosphate monobasic
LC3B	Microtubule-associated protein 1A/1B-light chain 3 B
LCAT	Lecithin-cholesterol acyltransferase
LDL	Low Density Lipoprotein
LPS	Lipopolysaccharide
lysoPC	Lysophosphatidylcholine
MAP1LC3	Microtubule-associated protein 1A/1B- light chain 3
MCP-1	Monocyte chemoattractant protein 1
MFI	Mean Fluorescence Intensity
µg	Microgram
mg	Milligram
min	Minutes
µl	Microliter
ml	Milliliter
µm	Micrometer
µM	Micromolar
mM	Millimolar
MMP	Mitochondrial membrane potential
mPTP	Mitochondrial permeability transition pore
mTOR	Mammalian target of rapamycin
mtROS	Mitochondrial Reactive Oxygen Species
MTT	3-(4,5-dimethylthiazol-2-yl)-2,5-diphenyl tetrazolium bromide
$Na_2HPO_4.12H_2O$	Sodium phosphate dibasic dodecahydrate
Na_3VO_4	Sodium orthovanadate

NaCl	Sodium chloride
NaF	Sodium fluoride
NaOH	Sodium hydroxide
NC	Nitrocellulose
ng	Nanogram
nm	Nanometer
nM	Nanomolar
OCR	Oxygen Consumption Rate
ox-LDL	Oxidized Low Density Lipoprotein
PBS	Phosphate-buffered saline
PBST	Phosphate-buffered saline Tween
PE	Phosphatidylethanolamine
PFA	Paraformaldehyde
PI3P	Phosphatidylinositol-3-phosphate
PMA	Phorbol-12-myristate-13-acetate
PMSF	Phenylmethylsulfonyl fluoride
PVDF	Polyvinylidene fluoride
RCT	Reverse Cholesterol Transport
RIPA	Radioimmunoprecipitation assay
RNA	Ribonucleic acid
ROS	Reactive Oxygen Species
SD	Standard Deviation
SDS	Sodium dodecylsulfate
SDS-PAGE	Sodium dodecylsulfate polyacrylamide gel electrophoresis
SQSTM1	Sequestosome-1
SR-B1	Scavenger Receptor Class B Type 1
SSC	Side Scatter
TCA	Tricarboxylic acid
TEMED	Tetramethylethylenediamine
TNF-α	Tumor necrosis factor alpha
V	Volts

LIST OF FIGURES

LIST OF TABLES

ÖZET

Yüksek Yoğunluklu Lipoproteinin (HDL) Monositik Hücre Hattında Otofaji ve Mitokondriyal İşlevler Üzerine Etkisi

Ateroskleroz gibi metabolik hastalıklarda otofaji mekanizmasının, mitokondriyal işlev bozukluklarının ve reaktif oksijen türleri (ROS) üretiminin önemli olduğu bilinmektedir. Ateroskleroz gelişiminde kritik role sahip monositlerin enerji metabolizmasına göre işlevinin değiştiği, bu değişikliğin sonucu olarak pro-inflamatuvar ya da anti-inflamatuvar fenotipe polarize olduğu bildirilmiştir. Yüksek Yoğunluklu Lipoprotein (HDL) anti-aterojenik işlev görerek ateroskleroz riskini azaltır. HDL'nin mitokondriyal hasarı azaltan antioksidan özelliklere sahip olduğu ve otofaji ile ilişkisi gösterilmiş olsa da, çalışma mekanizması bilinmemektedir. Bu çalışmada, HDL'nin U937 monositik hücre hattında otofaji, otofajik akı, mitokondriyal dinamikler ve ayrıca monositlerin farklılaşması üzerindeki etkisinin araştırılması amaçlandı. Bu amaç doğrultusunda, U937 hücreleri HDL ile muamele edildikten sonra otofajik akı, otofaji belirteçleri LC3B ve p62 protein seviyelerinin western blot yöntemiyle analizi sonucu incelendi. Mitokondriyal dinamikler, akış sitometrisi ve konfokal görüntüleme ile değerlendirildi. Oksijen tüketim hızı (OCR), Seahorse XFp Cell Mito Stress Kit ile ölçüldü. Makrofaj polarizasyon belirteçleri, PMA ile makrofaja farklılaştırılan U937 hücrelerinde HDL varlığında ve yokluğunda analiz edildi. Sonuçlar, HDL ile muamele edilmiş U937 hücrelerinde LC3B protein seviyelerinde artış ortaya çıkardı. HDL muamelesi mitokondriyal kütle ve mitokondriyal membran potansiyelinde azalmaya neden oldu. HDL ile muamele edilen hücrelerde mitokondriyal solunum azaldı. Ek olarak, M2 fenotip belirteçleri olan CD163 ve CD206, farklılaşmış hücrelerde HDL muamelesi ile arttı. Bu çalışma, HDL'nin monositlerde otofaji ve makrofaj polarizasyonu üzerindeki etkisini gösteren ilk çalışmadır. Bulgular HDL'nin aterosklerozdaki koruyucu rolünü bu mekanizmaların düzenlenmesi ile gerçekleştirebileceğini işaret etmektedir.

Anahtar Sözcükler: HDL, otofaji, mitokondriyal dinamikler, makrofaj polarizasyonu, doğal bağışıklık.

ABSTRACT

The Effect of High Density Lipoprotein (HDL) on Autophagy and Mitochondrial Dynamics in a Monocytic Cell Line

Autophagy mechanism, mitochondrial dysfunction and reactive oxygen species (ROS) production are key factors in metabolic diseases, including atherosclerosis. Monocytes, which are essential for the development of atherosclerosis, alter their function in response to energy metabolism. Thereby, they become polarized into pro-inflammatory or anti-inflammatory phenotypes. High Density Lipoprotein (HDL) serves as an anti-atherogenic agent and reduces the risk of atherosclerosis. Although HDL has been shown to have anti-oxidant properties that reduce mitochondrial damage, its working mechanism is unclear. This study aims to investigate the effect of HDL on autophagy, autophagic flux, mitochondrial dynamics and also on the differentiation of monocytes in the U937 monocytic cell line. For this purpose, protein levels of autophagy markers, LC3B and p62, were analyzed by western blotting in HDL treated U937 cells to determine autophagic flux. Mitochondrial dynamics were evaluated by flow cytometry and confocal imaging. Oxygen consumption rate (OCR) was measured by Seahorse XFP Cell Mito Stress Kit. Macrophage polarization markers were analyzed in PMA-differentiated U937 cells in the presence and absence of HDL. An increase in LC3B levels and a decrease in mitochondrial mass, mitochondrial membrane potential and mitochondrial respiration were observed in HDL treated cells. Furthermore, M2 phenotype markers CD163 and CD206 were increased upon HDL treatment in differentiated cells. This is the first study to demonstrate the effect of HDL on autophagy and macrophage polarization in monocytes. Our data indicate that HDL can achieve its protective role in atherosclerosis via regulation of these mechanisms.

Keywords: HDL, autophagy, mitochondrial dynamics, macrophage polarization, innate immunity.

1 INTRODUCTION AND AIM

The pivotal function of High Density Lipoprotein (HDL), is to take place in reverse cholesterol transport (RCT). HDL transports free cholesterol from macrophages in peripheral tissues to the liver for disposal (1). Apart from RCT, HDL also functions as a protective mechanism for the cell in innate immunity. HDL exhibits anti-atherosclerotic effects, including endothelial inflammation (2) and leukocyte activation reduction which are involved in atherosclerotic plaque development and progression (3). The increased HDL cholesterol (HDL-C) levels in the serum directly affects the macrophages formed in the lesion and contributes to atherosclerotic lesion regression (4).

Autophagy acts as a survival mechanism for organisms under stress by destroying damaged organelles, toxic protein aggregates and intracellular pathogens for the proper functioning of the immune system, providing protection against metabolic stress induced diseases, such as atherosclerosis (5). Selective lysosomal degradation of lipids provides free cholesterol to macrophages for cholesterol efflux. This shows the importance of autophagy for RCT, and indicates that the cell protective mechanisms of HDL and autophagy may intersect.

Mitochondria are essential for the energy production in the cell, but they also play an important role in the regulation of various cellular functions such as cell metabolism and response to oxidative stress. According to the physiological or pathological changes in the energy requirement of the cell, they can change their shape, oxidative phosphorylation capacity and function. Elimination of damaged mitochondria is crucial for cell survival. If damaged mitochondria are not eliminated properly, they can have harmful effects on cells. Damaged and dysfunctional mitochondria can cause cellular degeneration, leading to neurodegenerative, metabolic and cardiovascular diseases (6). Proper functioning of mitochondria plays an important role in the production of immune cells, their activity and the preservation of their phenotypic characteristics (7). Recent studies also indicate that immune cells may have different phenotypes depending on the change in mitochondrial function.

In this study, we aimed to examine the effects of HDL on autophagy in monocytes. Aside from this, we investigated the effect of HDL on mitochondrial dynamics in normal physiology and differentiated monocytes. For this purpose, U937 cells, a monocytic cell line, were treated in the presence and absence of HDL, and autophagy activation and autophagic flux were investigated by western blot. Surface antigens, which are differentiation markers, were analyzed by flow cytometry. In addition, mitochondrial membrane potential, mitochondrial SOX and mitochondrial mass were measured using mitochondria-specific dyes and mitochondrial respiration was examined by Seahorse XFp Analyzer.

It is well known that HDL serves a prominent anti-atherogenic function and reduces the risk of atherosclerosis. It is possible that the anti-atherogenic function may be due to autophagy activation and HDL may result in differentiation of monocytes into different macrophage phenotypes. This may lead to changes in mitochondrial dynamics during differentiation or polarization. Although it has been shown that HDL has anti-oxidant properties that reduce mitochondrial damage, the working mechanism on autophagy and mitochondrial dynamics is unknown.

2 BACKGROUND

2.1 High Density Lipoprotein

High Density Lipoprotein (HDL) acts a key anti-atherogenic factor by arbitrating reverse cholesterol transport (RCT). RCT is initiated by the binding of Apolipoprotein AI (apoA-I) in HDL particles, which are poor in lipid content with the ATP-binding cassette transporter A1 (ABCA1) on target cells such as macrophages. This grants HDL particles to operate as an acceptor for cholesterol. These poor in lipid content HDL can finally be converted to a mature HDL particle by lecithin-cholesterol acyltransferase (LCAT) activity. LCAT activation transforms HDL from an incipient disc shape to a matured spherical structure and hence increases the particle's capacity to carry cholesterol. Mature HDL is perceived to be mediating cholesterol efflux by interacting with the ABCG1 transporter (8,9). The continuous binding of HDL containing apoA-I to the scavenger receptor B1 (SR-B1) on hepatocytes allows cholesterol unloading which is then secreted as bile at the end of the cycle (10). By this mechanism, HDL decreases inflammation and reduces atheroma formation (11).

Other than RCT, HDL operates in innate immunity and longevity as a protective mechanism for the cell (12,13). HDL appears to implement anti-atherosclerotic effects by reducing endothelial inflammation and leukocyte activation, which are involved in the development and progression of atherosclerotic plaque (2,3). Increasing plasma levels of HDL cholesterol also appears to directly impact macrophages in the lesion and could contribute to atherosclerotic lesion regression (4). Proteomic studies have revealed the presence of more than 100 proteins associated with HDL in addition to apoA-I and apoA-II (14). Furthermore, HDL subsets containing different numbers and compositions of lipids suggest that HDL may serve specific biological roles. Although some of the HDL related proteins are specifically related to lipid transport, a large percentage has been shown to be related to protease inhibition, complement regulation, and acute phase response (15). These studies show that the function of HDL is too broad to be limited to lipid transport.

HDL's functions include providing an innate immune response, protecting vascular tone, limiting inflammation, regulating glucose metabolism, and having antiapoptotic effects (16). Prevention of lipoapoptosis in the artery wall, reduction of oxidative stress in plasma and cellular compartments, stimulation of cell proliferation *in vitro* by inhibiting the mitochondrial pathway of apoptosis are also among the effects of HDL (17) (Figure 1). Unraveling the functions of HDL in the near future reveals that HDL may be a potential tool as a therapeutic agent against cardiovascular diseases (1).

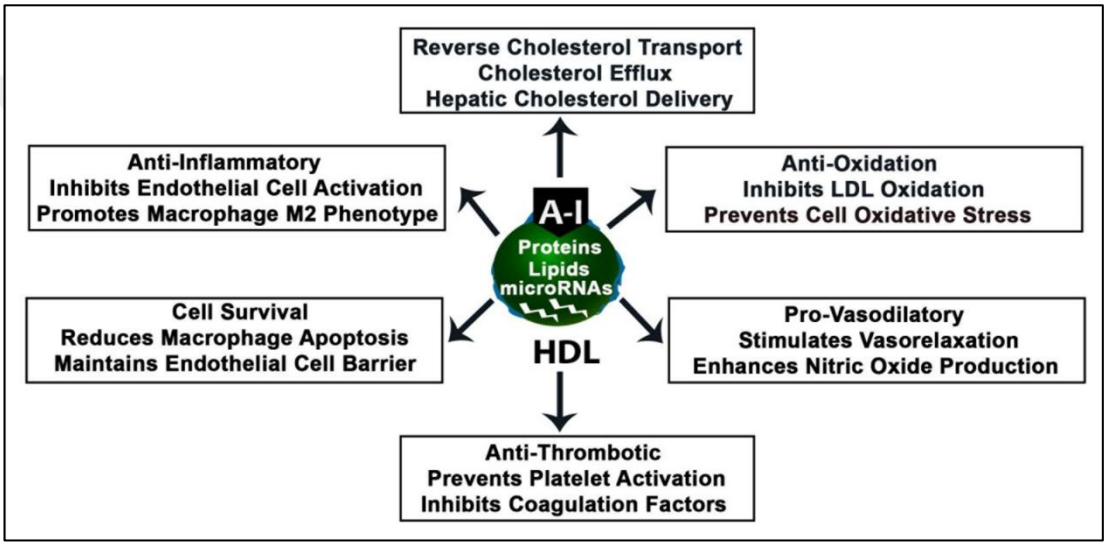

Figure 1. Various functions of HDL (13).

2.1.1 Relation between HDL-C levels and function

HDL cholesterol is the level of HDL in milligrams per deciliter of blood. According to The Adult Treatment Panel (ATP III) guidelines, when HDL cholesterol levels are <40mg/dl in men and <50m/dl in women, it is considered low and defined as a cardiovascular risk factor (18). Both genetic and environmental factors play a role in interpersonal differences in HDL-C levels. Environmental factors include smoking, lack of physical activity and diet with high triglyceride content. Increasing physical activity and weight loss increase HDL-C levels.

High HDL-C levels are known to be protective against atherosclerosis. It is traditionally known that each 1mg/dl decrease in HDL-C levels will increase the risk of coronary artery disease (CAD) by 2-3% (19). In recent years, this has been replaced by the view that the functionality of HDL is more important than HDL-C levels. The reason for this is that the relation between the effect of increased HDL-C levels. This is due to the fact that the relationship between the effect of increased HDL-C levels in CAD cannot always be studied in recent research on molecules that contribute to the maturation of HDL and take part in RCT. Additionally, some research indicates that there is no connection between atherosclerosis and low HDL levels in blood. ApoA-1 Milano is a very rare mutation that results in no cardiovascular risk even though the HDL-C levels are low. Furthermore, even the protective effect of this mutation against atherosclerosis has been reported in clinical studies (20). Studies in mice revealed that although the increase in SR-B1 decreases HDL-C levels, it increases the transport of cholesterol to the liver. This leads us to think that increased SR-B1 levels may be important in the treatment of atherosclerosis (21). Recent publications also point to a condition that's predisposed to dysfunction and systemic inflammation in men when HDL-C levels are too high (22). In addition, high HDL-C levels in patients with Type 1 diabetes do not protect the patient from CAD and indicates that HDL loses its protective properties on the vessel wall (23). There is a growing amount of publications examining the relationship between HDL-C levels and function. Since, the most critical step in which HDL functionality is decisive is macrophages, where RCT first begins, the literature claims that treatment strategies can be associated with macrophages (15,24).

2.2 Autophagy

Autophagy, like apoptosis, is one of the regulatory mechanisms that determine cell fate in disease and health. Autophagy is a process that recycles damaged organelles and cells in order to ensure cell survival. It plays a role in the degradation of misfolded or aggregated proteins, clearance of damaged organelles and elimination of intracellular pathogens (25). It is known that autophagy is involved in the selective destruction of large macromolecules such as protein and lipid clusters, and in the lysis

of damaged cell organelles. It is also related to various processes such as cell survival and inflammation. Under stress conditions, autophagy acts as a survival mechanism for the organism by destroying damaged organelles, toxic protein aggregates and intracellular pathogens for the proper functioning of the immune system. Moreover, it acts as a protector in metabolic stress-induced diseases (26). However, it has been revealed that autophagy is not only related to cell homeostasis in the last decade. Autophagy has also been shown to be effective in the regulation of metabolism, morphogenesis, cell differentiation, aging, cell death, and elimination of intracellular pathogens as part of the immune system (27). In addition, anomalies in autophagy may also be the cause of many multisystem diseases. It was observed that downregulating the expression of Atg5, Atg7, and Beclin1 also suppressed cell death (28,29).

A complex network of more than thirty genes and proteins control the autophagic mechanism (Figure 2). These are known as autophagy-related genes (Atgs) and autophagy-related proteins (ATGs). ATGs regulate the autophagy process by being responsible for the activation of autophagy, the formation and elongation of the autophagosome membrane, the orientation of the contents to the lysosome, and the fusion of the autophagosome and the lysosome membrane (30).

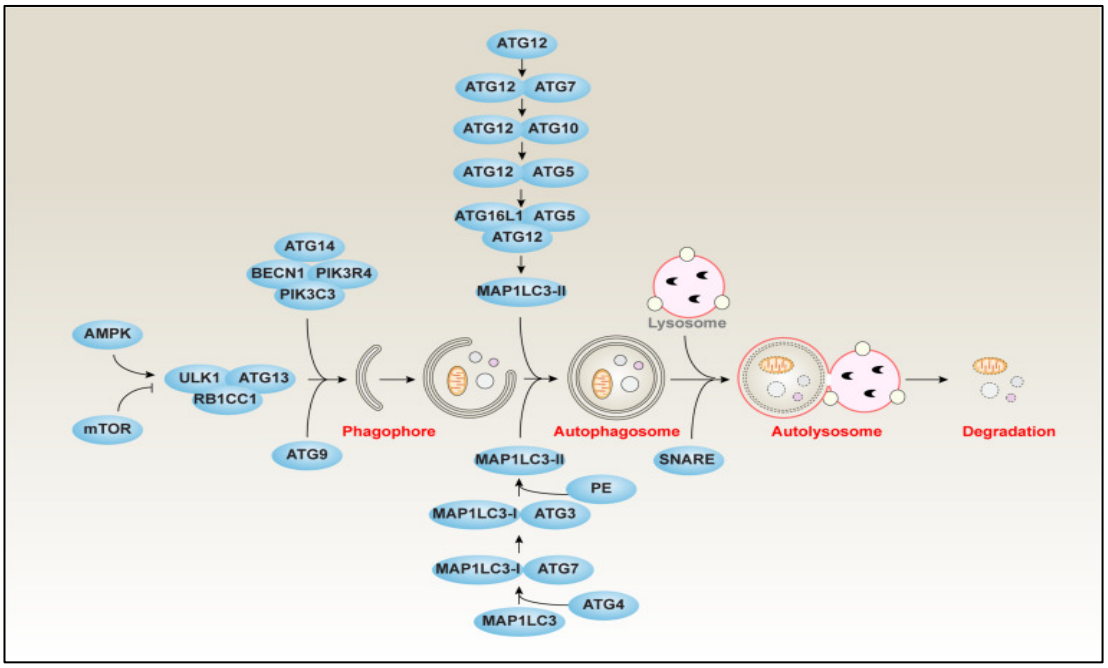

Figure 2. Core molecular mechanism of autophagy (5).

As a result of a stimulating signal in the autophagic mechanism, ATG1-13-17 protein kinase complex activates the phosphatidylinositol-3-phosphate (PI3P) kinase-BECN1 complex and initiates nucleation. The elongation and the vesiculation of the autophagosome membrane after nucleation, is controlled by two ubiquitin-like reactions. One of these is the binding of ATG5-ATG12 complex with ATG16 to the isolation membrane. This complex then triggers the assembly of ATG8/LC3 to phosphatidylethanolamine (PE) (5). Microtubule-associated protein 1 light chain 3 (MAP1LC3) is the human counterpart of yeast ATG8, and the formation of the autophagosome is dependent on the production of MAP1LC3-II (31). Thus, lysosomal assembly and degradation of the contents in the lysosome are completed (32). Building blocks such as amino acids and fatty acids that emerge after destruction by lysosomal enzymes are brought back into the cell for reuse (33).

2.3 Autophagy, Lipid Metabolism and HDL

Autophagosomes have the ability to selectively cleave lipid particles for delivery to lysosomes for lipolysis in fibroblasts and hepatocytes. This process has been named 'lipophagy' and the presence of lipophagy has been demonstrated in neurons, macrophages and adipocytes (34). Later studies emphasized that lipophagy is important not only for triglyceride metabolism, but also for cholesterol catabolism and efflux in macrophages (35,36). Lipophagy regulation overlaps with neutral lipolysis and autophagy regulation. The role of autophagy in lipid metabolism is not only limited to lipophagy, but also includes interaction with cytosolic lipolysis pathways, lipid droplets and lipoprotein transport. One of the known relationships of autophagy with lipoproteins; it is to ensure the degradation of Apolipoprotein B (ApoB) aggregates to vastly limit the secretion of dysfunctional LDL (37).

Lipids are the target of autophagic degradation. Autophagic activity is increased in insulin resistant obese patients (38). This shows us that autophagic differentiation is necessary during development, but also for the maintenance of adipose tissue volume and lipid storage in adulthood. In addition, free fatty acids stimulate

autophagy, indicating that autophagy acts as a defense mechanism to prevent intracellular lipid accumulation.

Cholesterol as a lipid molecule is a key constituent of the cell membrane, steroids and signaling molecules. Although all lipids are physiologically important, triglycerides and cholesterol usually contribute to the development of coronary artery disease. Lipoproteins maintain the transport of these endogenous triglycerides and cholesterol. LDL circulates constantly in the blood until its cholesterol is absorbed by the tissues in the periphery, which causes a deposit of cholesterol. HDL ensures the excretion by the liver while carrying cholesterol from peripheral tissues. Defects in lipoprotein synthesis, processing and clearance pathways may lead to the accumulation of atherogenic lipids in plasma and endothelium. Factors that trigger hepatic lipoprotein synthesis usually lead to elevated plasma cholesterol levels (39). The elevation patterns in lipids and lipoproteins may create and imbalance which results in dyslipidemia. Dyslipidemia is the increase of total plasma cholesterol or lower HDL-C levels which ensues atherosclerosis development. The causes may be genetic or lifestyle choices such as alcohol overuse and also other diseases such as chronic kidney disease and hypothyroidism. Dyslipidemia by itself alone often causes no symptoms but it can lead to coronary artery disease, stroke and peripheral arterial disease (40).

Cellular cholesterol modifications are also important in autophagy regulation. Current research indicates a very immediate and intricate relationship between autophagy and dyslipidemia. The difference in intracellular lipid content affects the autophagy levels in cells. Short-term lipid stimulation can significantly promote autophagy, while long-term or specific types of lipid stimulation can inhibit autophagy levels (41). Decreased cholesterol stimulates autophagy in many cell types by inhibiting mTOR complex involved in cell growth and metabolic processes. An increase in the number of LC3 molecules bound with PE which indicates active autophagy and an increase in the number of autophagosomes were observed in various cell types with reduced cholesterol in the medium. Conversely, hypercholesterolemia suppresses autophagy by activating mTOR signaling. Cholesterol is carried in the blood by apolipoproteins (LDL, HDL). Oxidized-LDL increases autophagy by

increasing endoplasmic reticulum (ER) stress in macrophages and this process is inhibited by the presence of HDL (42). Intracellular Ca^{2+} increases and cell death occurs. Inhibition of autophagy promotes ER stress, mitochondrial dysfunction and lipid accumulation (43–45). On the contrary, activation of autophagy can reduce metabolic syndrome-associated diseases.

It is indicated that the most critical cells in cholesterol reflux are the macrophages. Lipid mobilization in macrophages is regulated by autophagy. Since macrophages are the key players in the formation of atherosclerosis, understanding how autophagy is regulated in these cells during lipid mobilization can shed light on the pathogenesis of atherosclerosis. Although accelerating autophagy in macrophages is considered as a new method to prevent atherosclerosis, autophagy may also begin as an inflammatory response in the vessel wall. Autophagy and HDL are thought to serve the same purpose in reducing oxidative stress (46). This means autophagy and HDL have a parallel action in cell protection. However, how HDL levels affect autophagy remains unknown.

2.4 Mitochondrial Dynamics and HDL

The mitochondrion is an energy producing organelle that produces ROS and heat as byproducts of oxidative phosphorylation. They also play an important role in the regulation of various cellular functions, including metabolism, response to oxidative stress, and steroid metabolism. Moreover, mitochondria are highly dynamic organelles. They tend to move along the cytoskeletal tracks and show varying morphology depending on the cell environment. These specific characteristics of mitochondria define mitochondrial dynamics which refer to mitochondrial biogenesis, fission and fusion events (47).

Mitochondrial fission and fusion are essential for maintaining their functioning state when cells are under metabolic or environmental stress. Mitochondrial fission ensures the correct division of mitochondria during mitosis to supply equal number of mitochondria to newly formed cells. It also involves the fragmentation of the critically

damaged mitochondria into small spherical organelles which are then eliminated by mitophagy. On the other hand, mitochondrial fusion defines the union of both inner and outer membranes of two nearby mitochondria in order to repair damaged parts of the organelle (48). Under healthy conditions, mitochondria tend to elongate by fusion to secure mitochondrial integrity and function which protects mitochondrial DNA from damage. During fusion, both mitochondria's proteins, lipids, and DNA are combined. This provides to clear the accumulation of mutations and mitochondrial ROS. Any hindrance in the fusion event can result in mitochondrial membrane potential loss, which damages mitochondria fitness (49). Studies elucidate the essential role of mitochondrial dynamics in the development of atherosclerosis. Recent data suggest that fission inhibition or fusion stimulation may offer a new therapeutic approach to reduce atherosclerosis progression (50).

The mitochondria are exposed to a lot of ROS because of their function in energy synthesis. It has been shown that under normal physiological conditions some electrons may escape from the electron transport chain during oxidative phosphorylation and react with oxygen to form superoxide anion. Complexes I and III are the principal sources of ROS during oxidative phosphorylation (51). At low production levels, ROS can act as signaling molecules. However, when produced in excess, ROS induce peroxidation of cellular lipids and proteins, damage mitochondrial and nuclear DNA and impair cell division. As a result, mitochondrial oxidative phosphorylation is significantly impaired. In addition, excessive ROS production causes mutations in mitochondrial DNA and protein misfolding and then leads to mitochondrial damage. Elimination of damaged mitochondria is crucial for cell survival. If damaged mitochondria cannot be removed properly, it can cause harmful effects on cells. Damaged and dysfunctional mitochondria can result in cellular degeneration, leading to serious disorders such as neurodegenerative, metabolic and cardiovascular diseases (6) (Figure 3).

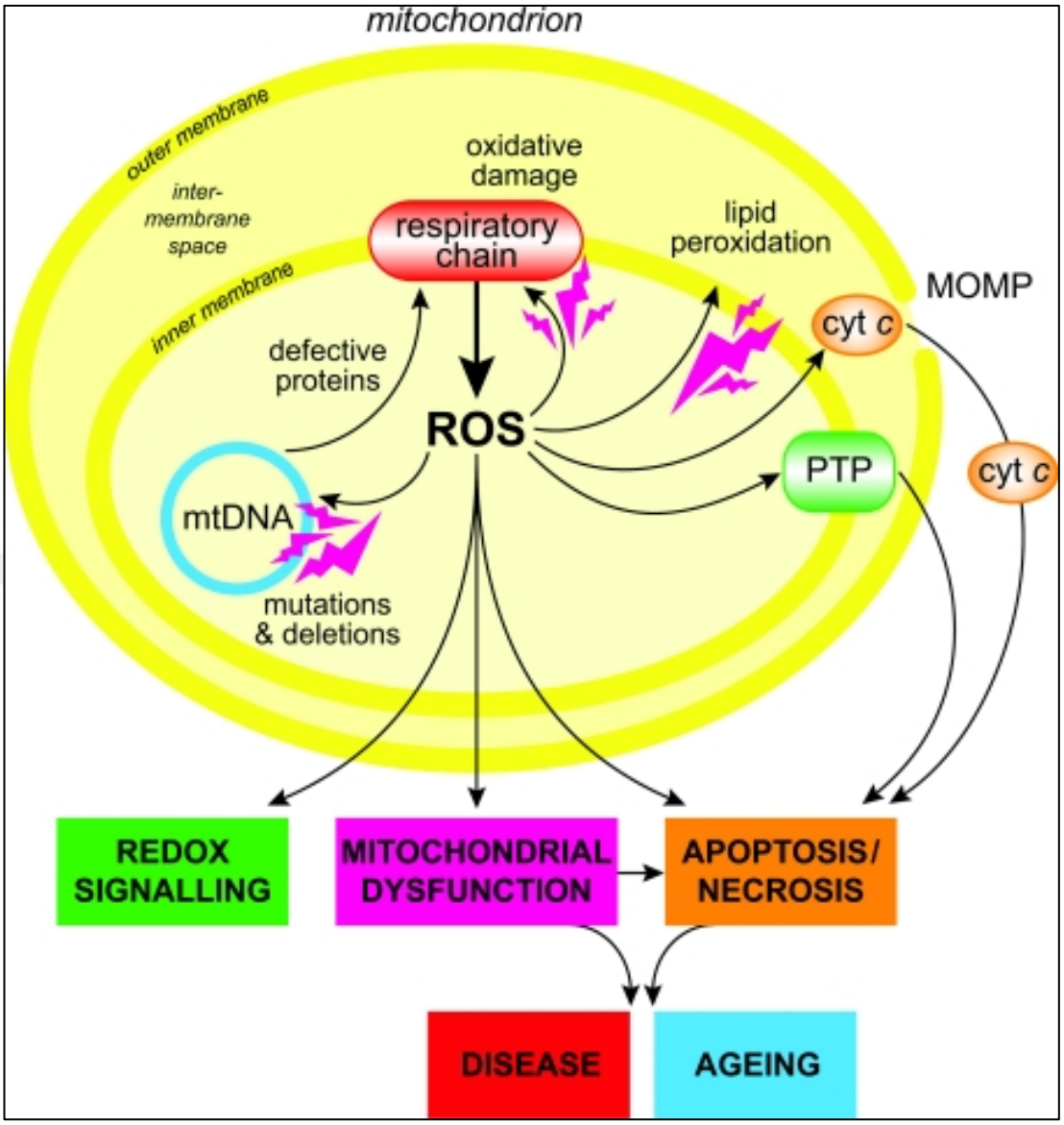

Figure 3. Mitochondrial ROS production (52).

Studies have shown that the increase in serum cholesterol and triglyceride levels is effective in mitochondrial dysfunction. In healthy cells and isolated mitochondria, lysophosphatidylcholine (lysoPC), a pro-inflammatory lipid associated with oxidized LDL, generates mitochondrial ROS production and enhances membrane permeability (53). Thus, the increase in oxidant formation damages the structure of the mitochondria. It impairs respiration by reducing oxidative phosphorylation and ATP production (54). Irreversible damage develops upon disruption of the mitochondrial membrane potential and opening of the mitochondrial permeability transition pore (mPTP).

Mitochondrial dysfunction in endothelial cells is induced by mitochondrial ROS generation, which is linked to increase of ox-LDL. LDL and its oxidized forms are a well-known risk factor for atherosclerosis. LDL first infiltrates the subendothelial space and becomes oxidized and then triggers an inflammatory reaction of the endothelium allowing the recruitment of monocytes within the arterial wall. Monocyte adhesion is typically thought to be the first step in the formation of atherosclerotic plaque. Differentiation of monocytes into macrophages allows these cells to internalize and accumulate oxidized LDL and become foam cells. Foam cells also synthesize pro-inflammatory mediators and growth factors that induce the smooth muscle cell proliferation (55). Furthermore, monocytes differentiated into macrophages migrate from the media to the intima of the artery wall and in return begin to secrete cytokines and growth factors. Some of the foam cells are loaded with cholesterol and contribute to the formation of the lipid core of the plate. Others proliferate and secrete extracellular matrix proteins around the foam cells to develop the fibrous cap of the plate (56,57). All these events combined lead to atherosclerosis and may cause plaque rupture (54) (Figure 4). The atherogenesis is also altered by the protective role of HDL. HDL has anti-inflammatory and antioxidant properties that protect mitochondria from damage, but its mechanism of action is unknown.

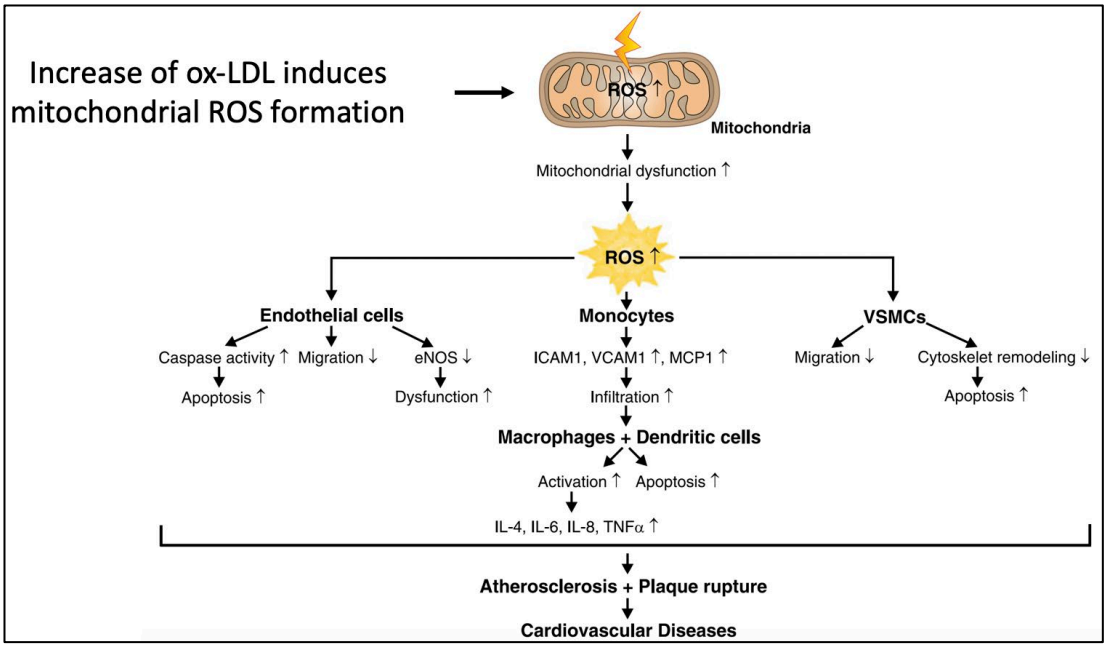

Figure 4. Role of mitochondrial ROS in atherosclerosis (54).

2.5 Immunity and HDL

The immune system can be thought of as a complex network in which many different cells and tissues work in harmony against pathogens. The regulation of this system takes place in many stages, and classically it occurs by sending the signal received from the receptors on the cell surface to the cell nucleus. Many recent studies have revealed that energy metabolism in the cell plays a role in the regulation of the immune system. Proper functioning of mitochondria is essential for the production of immune cells, the preservation of their phenotypic characteristics and their activities (7). If mitochondrial damage is eliminated by mitophagy, it causes hyperactivation of the inflammation pathway and then resulting in the development of chronic inflammation and inflammatory disorders (58).

Monocytes and their tissue counterpart macrophages, have a key role in the formation of pro-inflammatory and anti-inflammatory responses. Following recognition of pathogens by innate immunity receptors, inflammatory cytokines are released. Among these cytokines, IFN-γ leads to polarization of macrophages to inflammatory type called M1 macrophages. Macrophages stimulated by cytokines such as IL-4 and IL-13 are polarized to anti-inflammatory M2 macrophages. The different phenotypes of these cells result from a stable coordination of glycolysis, pentose phosphate pathway, fatty acid oxidation, mitochondrial oxidative phosphorylation, and TCA cycle (Figure 5).

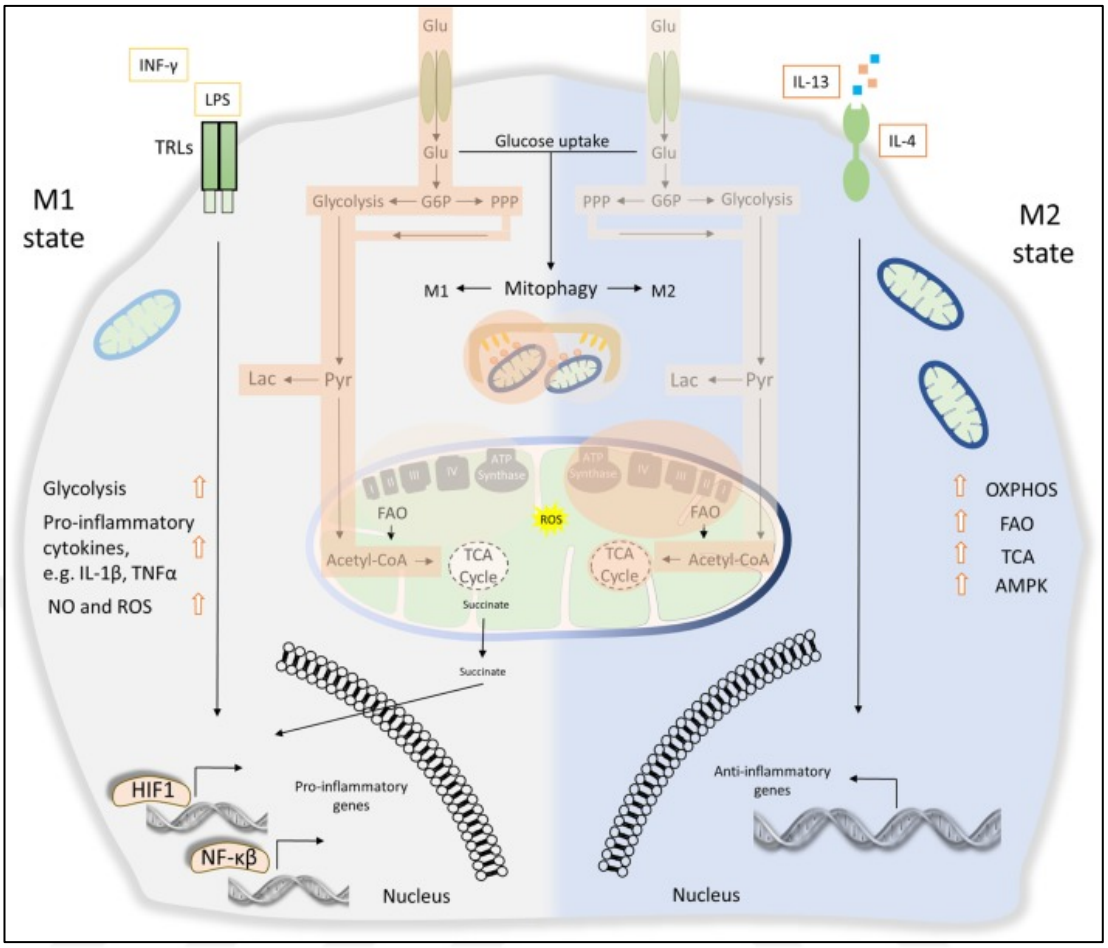

Figure 5. Metabolic makeup of M1 and M2 polarization (58).

Mitochondrial ROS (mtROS) which is a product of mitochondrial metabolism is involved in innate immunity feedback and macrophage activity. MtROS production has been observed to moderate inflammatory cytokine release (59). Correspondingly, various studies show that high mtROS levels are required for the bactericidal activity of macrophages to be effective (60). Again, recent studies reveal the importance of mitophagy in the regulation of the inflammatory response.

All these observations suggest that increasing HDL concentrations in serum and functional properties of HDL may be an important therapeutic agent to minimize mitochondrial damage. Recent studies with HDL have shown that HDL reduces the expression of M1 phenotype-specific cell surface markers CD64 and CD192 in macrophages. Also, the expression of M1 phenotype inflammatory genes TNF-α, IL-6 and MCP-1 have been reduced. Thereby, macrophage polarization to the M1

phenotype was inhibited by reducing ROS production (61). In another study, HDL treated mouse primary macrophages exhibited increased gene expression for the M2 phenotype markers Arginase-1 and Fizz-1, induced by IL-4. HDL also suppressed the expression of inflammation related genes in response to IFN-γ (62). These results made us think that HDL may be effective in M1/M2 macrophage differentiation. Recent studies also demonstrate that immune system cells may have different phenotypes depending on the changes in mitochondrial function.

3 MATERIALS AND METHODS

3.1 Materials

Table 1. List of reagents and suppliers

Antibodies	
Alexa Fluor 488-conjugated goat anti-rabbit IgG (H+L)	ThermoFisher Scientific
APC anti-human CD86	Sony Biotechnology
APC Mouse IgG1, κ Isotype Ctrl (FC)	Sony Biotechnology
FITC anti-human CD11c	Sony Biotechnology
FITC anti-human CD206 (MMR)	Sony Biotechnology
FITC Mouse IgG1, κ Isotype Ctrl (FC)	Sony Biotechnology
Mouse monoclonal anti-B-Actin Antibody (AC-74)	Sigma Aldrich
PE anti-human CD163	Sony Biotechnology
PE anti-human CD64	Sony Biotechnology
PE Mouse IgG1, κ Isotype Ctrl (FC)	Sony Biotechnology
Rabbit polyclonal anti-LC3B	Sigma Aldrich
Rabbit polyclonal anti-p62/SQSTM1	Novus Biologicals
Peroxidase affinipure goat anti-mouse IgG (H+L)	Jackson ImmunoResearch
Peroxidase affinipure goat anti-rabbit IgG (H+L)	Jackson ImmunoResearch
Dyes	
MitoSOX Red Mitochondrial Superoxide Indicator	ThermoFisher Scientific
MitoTracker Green FM	ThermoFisher Scientific
MitoTracker Red CMXRos	ThermoFisher Scientific
NucBlue Reagent (Hoechst 33342)	ThermoFisher Scientific
Kits	
µ-Slide 8 Well	Ibidi
µ-Slide VI 0.4	Ibidi
Cell Proliferation Kit I (MTT)	Roche
Seahorse XFp Cell Mito Stress Kit	Agilent Technologies
Chemicals	
0% Fat skim milk	Régilait
2-mercaptoethanol	Sigma Aldrich
30% Acrylamide/Bis-acrylamide	Serva
Acetic acid	Sigma Aldrich
Amersham Hybond P 0.2 PVDF membrane	GE Healthcare
Amersham Protran 0.2 NC membrane	GE Healthcare
Ammonium persulphate	Sigma Aldrich
Bafilomycin A1	Enzo
Beta-Mercaptoethanol	BioRad
Bovine Serum Albumin (BSA) Fraction V	Roche
Bradford Reagent 5X	Serva
Bromophenol Blue	Sigma Aldrich
Complete EDTA-free protease inhibitor cocktail	Roche
Dimethyl sulphoxide (DMSO) Hybri-Max	Sigma Aldrich
DTT	Applichem
Ethanol	Sigma Aldrich
Ethylenediaminetetraacedic acid (EDTA)	Sigma Aldrich
Glycerol	Sigma Aldrich
Glycine	Merck
Glucose monohydrate	Sigma Aldrich

Table 1. List of reagents and suppliers (continued)

HI Fetal Bovine Serum (FBS)	Gibco
High Density Lipoprotein (HDL)	Lee Biosolutions
Hydrochloric acid	Sigma Aldrich
Igepal CA-630	Sigma Aldrich
Lipopolysaccharides from Escherichia coli	Sigma Aldrich
Methanol	Sigma Aldrich
PageRuler Plus Prestained Protein Ladder, 10 to 250 kDa	ThermoFisher Scientific
Paraformaldehyde	Sigma Aldrich
Penicilin-Streptomycin	Gibco
Phenylmethanesulfonyl (PMSF)	Applichem
Phorbol-12-myristate-13-acetate (PMA)	Sigma Aldrich
Phosphate Buffer Saline (PBS) (1X)	Gibco
Ponceau S	Sigma Aldrich
Potassium chloride	Sigma Aldrich
Potassium dihydrogen phosphate	Sigma Aldrich
RPMI 1640 Medium	Gibco
Sodium dodecyl sulfate	Sigma Aldrich
Sodium azide	Sigma Aldrich
Sodium chloride	Sigma Aldrich
Sodium fluoride	Sigma Aldrich
Sodium hydroxide	Merck
Sodium orthovanadate	Sigma Aldrich
Sodium phosphate dibasic dodecahydrate	Sigma Aldrich
Sodium Pyruvate 100mM (100X)	Gibco
SuperSignal West Pico Chemiluminescent Substrate	ThermoFisher Scientific
TEMED	Sigma Aldrich
Torin 1	SelleckChem
Triton X-100	Sigma Aldrich
Trizma Base	Sigma Aldrich
Trypan Blue Solution	Sigma Aldrich
Tween-20	Sigma Aldrich
Western blotting filter paper extra thick paper	ThermoFisher Scientific
Equipement	
+4°C fridge	Kirsch
-20°C freezer	Kirsch
-80°C freezer	Haier
Biosafety cabinet	ThermoFisher Scientific
Cell culture incubator	Esco
ChemiDoc MP Imaging System	BioRad
Confocal microscope	Zeiss LSM 700
Flow cytometer	BD FACSVerse
Inverted microscope	Zeiss
Micro centrifuge	ThermoFisher Scientific
Mini centrifuge	Biosan
Nitrogen tank	ThermoFisher Scientific
Plate reader	BioTek
Rocker shaker	Witeg
Seahorse XFp Analyzer	Agilent Technologies
Trans-blot Turbo Transfer System	BioRad
Varioskan Flash	ThermoFisher Scientific
Ventilated micro centrifuge	ThermoFisher Scientific
Water bath	Nüve

3.1.1 Preparation of chemicals for cell culture

High Density Lipoprotein (HDL) (100mg)

30µl aliquots of 100mg HDL were prepared and stored in -80°C. Working stock was freshly prepared with RPMI medium for 20, 50 and 100µg/ml treatment conditions. Treatments were followed for 4, 16 and 24 hours at 37°C.

Bafilomycin A1 (160µM)

100µg vial was dissolved in 1,0035ml DMSO to prepare 160µM stocks. Main stock was filtered by a 0,22µm filter and 20µl aliquots were stored in -80°C. 10µM working stock was freshly prepared with RPMI medium and 25nM treatment was carried for 2 hours at 37°C.

Torin 1 (1mM)

2,2mg Torin 1 was dissolved in 3,6244ml DMSO in order to obtain 1mM stocks. The stock solution was filter sterilized with a 0,22µm filter. 10µl aliquots were taken and stored in -80°C. 10µM working stock was freshly prepared with RPMI medium and 100nM treatment was carried for 2 hours at 37°C.

PMA (160µM)

The vial is dissolved in DMSO in order to obtain 1mg/ml main stock. 10µl aliquots were taken and stored in -20°C. 16,21µM working stock was freshly prepared with RPMI medium and 40nM treatment was carried for 48 hours at 37°C.

LPS (1mg/ml)

1mg LPS was dissolved in 1ml sterile ddH_2O to obtain the main stock which was stored in -20°C. 100ng/ml treatment was carried for 24 hours at 37°C.

3.1.2 Gels, buffers and solutions

Table 2. 15% Polyacrylamide separating gel (5ml)

30% Acrylamide/Bis-acrylamide	2,5ml
1,5M Tris (pH: 8,8)	1,25ml
50% Glycerol	375µl
ddH_2O	875µl
10% APS	50µl
TEMED	5µl

Table 3. 12% Polyacrylamide separating gel (5ml)

30% Acrylamide/Bis-acrylamide	2ml
1,5M Tris (pH: 8,8)	1,25ml
50% Glycerol	375µl
ddH_2O	1,375ml
10% APS	50µl
TEMED	5µl

Table 4. 4% Polyacrylamide stacking gel (2,5ml)

30% Acrylamide/Bis-acrylamide	325µl
1M Tris (pH:6.8)	625µl
20% SDS	12,5µl
ddH_2O	1,512ml
10% APS	12,5µl
TEMED	5µl

10X Tris-Glycine Running Buffer (pH 7,4 – 8,5)

- 0,25M Tris
- 1,92M Glycine
- 1% SDS
- 10X running buffer is diluted to 1X with ddH2O

10X Bjerrum Schafer-Nielsen Transfer Buffer (pH 9,2)

- 48mM Tris

- 39mM Glycine
- 20% methanol
- 10X transfer buffer is diluted to 1X with ddH2O and 20% methanol

10X PBS (pH 7,4)

- 1,37M NaCl
- 30mM KCl
- 35mM KH_2PO_4
- 0,1M $Na_2HPO_4.12H_2O$
- 10X PBS is diluted to 1X with ddH2O

1X PBST

- 1X PBS
- %0,5 Tween-20

1X RIPA Lysis Buffer

- 50mM Tris-HCl (pH 7,4)
- 150mM NaCl
- 1mM EDTA
- 1mM NaF
- 1mM Na_3VO_4
- 0,5% Igepal CA-630
- 0,5% Triton X-100
- 0,5mM PMSF in ethanol
- 1mM DTT

5X Laemmli Loading Buffer

- 250mM Tris-HCl (pH 6,8)
- 50% Glycerol
- 5% SDS
- 1% Bromophenol Blue

- 5% Beta-Mercaptoethanol

1% Bromophenol Blue

- 100mg Bromophenol Blue
- 10ml methanol
- Vortexed and then filtered

Ponceau S

- 0,1% (w/v) Ponceau S
- 5% Acetic acid

5% Skimmed Milk

- 5% (w/v) skimmed milk prepared in 1X PBST

5% BSA for primary antibodies

- 5% (w/v) Fraction V BSA
- 0,02% Sodium azide

25X Protease Inhibitor

1 tablet of Roche cOmplete EDTA-free protease inhibitor cocktail was dissolved in 2ml sterile ddH_2O to obtain 25X stock. 50µl aliquots were taken and stored at -20°C. 1X dilution was freshly prepared with RIPA lysis buffer before preparing cell lysates.

4% PFA for immunofluorescence

20g paraformaldehyde was dissolved in 500ml 1X PBS. pH of the solution was set to 7,2 with NaOH. Solution was filter sterilized using 0,22µm filter. 10ml aliquots were taken and stored at -80°C.

Permeabilization Buffer

0,2% Triton X-100 in dPBS was filter sterilized using 0,2µm filter.

Blocking and Antibody Dilution Buffer

0,1% Triton X-100 and 2mg/ml BSA in dPBS was filter sterilized using 0,2µm filter.

Washing Buffer

0,1% Triton X-100 in dPBS was filter sterilized using 0,2µm filter.

3.2 Methods

3.2.1 Cell culture

U937 monocyte cells (ATCC, CRL-1593.2) were cultured in RPMI 1640 medium supplemented with 1% penicillin-streptomycin and 10% heat inactivated sterile fetal bovine serum (FBS) in a humidified atmosphere of 5% CO_2 at 37°C. The medium was changed every 2-3 days. Cells were passaged to $2x10^5$ cells/ml when they reached $1x10^6$ cells/ml. In all experiments, cells were seeded in complete RPMI medium.

3.2.2 Cell proliferation assay

U937 cells were seeded at $1x10^4$ density in a 96-well plate. Cells were incubated in triplicate with increasing concentrations of HDL (20, 50 and 100µg/ml) including a control group (only medium) for 4, 16 and 24 hours at 37°C. Cell viability was measured using the MTT Kit I (Roche) following manufacturer's protocol. Absorbance was measured at 570nm using an ELISA reader with a reference serving as blank. Control cells were taken as 100% and HDL treated cells were analyzed according to control.

3.2.3 Protein isolation

Prior to seeding, cell medium was changed the day before. U937 cells were seeded $5x10^5$/ml in a 12 well plate. The cells were treated with or without 100µg/ml HDL for 16 hours. 100nM Torin 1 and 25nM bafilomycin treatments were followed for 2 hours. Cell pellets were collected from each sample and washed once with dPBS. Then, the pellets were lysed with 1X RIPA lysis buffer. For this purpose, pellets were dissolved in 50µl RIPA buffer and incubated on ice for 10 min. After pipetting gently, another incubation on ice for 10 min was followed. Later, cells were centrifuged at 14000 rpm at 4°C for 10 min. Supernatants were transferred into new tubes and protein samples were stored at -80°C.

3.2.4 Protein concentration determination

Protein concentrations were determined by Bradford Assay using BSA as a standard. For this purpose, 1, 0,5, 0,25, 0,125, and 0,0625µg/µl BSA standards were prepared by serial dilution to create a standard curve. Each protein was diluted in sterile dH_2O at 1:10 ratio. 10µl of each sample and BSA standard were put into a 96-well plate in triplicates. Sterile dH_2O was used as blank. 190µl of 1X Bradford reagent was added into each well and samples were incubated at dark for 5 min at room temperature. After 5 min, plate is read at 595nm. Mean values of each sample and BSA standards were calculated. Protein concentrations were calculated according to the equation obtained from BSA standard curve.

3.2.5 SDS-PAGE and western blotting

5X Laemmli loading buffer was diluted to 1X with 50µg protein sample and heated at 95°C for 5 min. Samples were loaded to 12-15% polyacrylamide gels and run at 80V for 45 min then, at 100V until the samples reached the bottom of the gel. The 12% gel was transferred to nitrocellulose membrane for 45 min and the 15% gel was transferred to 0,2µm PVDF membrane for 30 min by BioRad trans-blot semi dry blotting system. After transfer, Ponceau S dye was used to stain the nitrocellulose

membrane to check whether proteins were transferred successfully. The membrane was blocked with %5 skimmed milk solution for 1 hour at room temperature. Afterwards, membranes were probed with rabbit anti-LC3B (1:5000), rabbit anti-p62 (1:2000) and mouse anti-β-actin (1:10000) primary antibodies overnight at 4°C. The following day, membranes were washed three times with PBST for 7 min at room temperature. Later, membranes were probed with peroxidase- conjugated anti-rabbit (1:10000) or anti-mouse (1:10000) secondary antibodies for 1 hour at room temperature. Membranes were then washed three times with PBST for 7 min and SuperSignal West Pico chemiluminescent solution was applied for 3 min onto membranes for imaging. The images were obtained by BioRad ChemiDoc instrument and analyzed using ImageLab software.

3.2.6 Immunofluorescence staining

Prior to seeding, cell medium was changed the day before. U937 cells were seeded $5x10^5$/ml in a 6 well plate. The cells were treated with or without 100µg/ml HDL for 16 hours. Cells to be analyzed were pelleted by centrifugation at 500xg for 5 min. The growth medium supernatant was aspirated and replaced with dPBS at a concentration of ~$5x10^5$cells/250µl and transferred to an ibidi µ-Slide 8 well plate. The ibidi µ-Slide plate was then left stationary for 30 min at room temperature to allow for sedimentation and adhesion of cells onto the well bottom. Adherent cells were then fixed for 20 min at room temperature with 4% PFA. Fixed cells were washed once with dPBS for 5 min before being permeabilized for 10 min. Permeabilized cells were washed once again with dPBS for 5 min and were then blocked with blocking buffer for 30 min at room temperature. The blocking solution was replaced with anti-rabbit LC3B (1:500) primary antibody diluted in antibody dilution buffer and left to incubate overnight at 4°C. Cells were subsequently washed 3 times for 5 min and incubated with the AF 488-conjugated anti-rabbit (1:1000) secondary antibody diluted in antibody dilution buffer for 1 h at room temperature, protected from light. Cells were again washed 3 times with dPBS for 5 min. At this point, nuclei were counterstained with the NucBlue dye at a working dilution for 10 min and then washed twice with dPBS for 5 min to

remove excess dye. Images were taken with 40x objective using Zeiss LSM 700 confocal microscope and images were analyzed by ImageJ software.

3.2.7 Evaluation of mitochondrial dynamics by confocal microscopy

The cells used in mitochondrial staining were incubated and prepared in the same manner as in immunofluorescence experiments. $5x10^5$ cells from each group were stained with 50nM MitoTracker Red CMXRos, 5μM MitoSOX Red and 100nM MitoTracker Green FM for 20 min at 37°C. After 20 min, samples were washed with dPBS. Cells were then transferred into an ibidi μ-Slide VI 0.4 chamber. Images were taken with 40x objective using Zeiss LSM 700 confocal microscope and corrected total cell fluorescence (CTCF) of 50 cells were analyzed using ImageJ software.

3.2.8 Evaluation of mitochondrial dynamics by flow cytometry

Prior to seeding, cell medium was changed the day before. U937 cells were seeded $5x10^5$/ml in a 6 well plate. The cells were treated with 100μg/ml HDL for 4, 16, 24 hours. After treatment, cells were harvested and centrifuged at 500xg for 5 min. Pellets were dissolved in 50μl dPBS and $3x10^5$ cells from each group were stained with 100nM MitoTracker Red CMXRos, 5μM MitoSOX Red and 100nM MitoTracker Green FM for 20 min at 37°C to determine mitochondrial membrane potential, mitochondrial superoxide formation and mitochondrial mass respectively. After 20 min, samples were washed once with dPBS. Pellets were dissolved in 400μl dPBS and transferred to flow cytometry tubes. Samples were analyzed by BD FACSVerse instrument. A total of $1x10^4$ events were acquired, gated and analyzed using the BD FACS Suite software.

3.2.9 Evaluation of macrophage polarization by flow cytometry

Prior to seeding, cell medium was changed the day before. U937 cells were seeded $5x10^5$/ml in 6cm petri dishes. Macrophage differentiation with PMA was initiated for 48 hours. After differentiation, U937 cells were incubated for 24 hours in the presence

of 100ng/ml LPS, 100µg/ml HDL, and both LPS and HDL. After these treatments, cells were harvested and centrifuged at 500xg for 5 min. Pellets were dissolved in 50µl dPBS and $15x10^4$ cells from each group were incubated with macrophage marker CD11c for positive control, CD64 and CD86 for M1 phenotype, and CD163 and CD206 surface marker antibodies for M2 phenotype for 20 min at 37°C. After 20 min, samples were washed once with dPBS. Pellets were dissolved in 400µl dPBS and transferred to flow cytometry tubes. Samples were analyzed by BD FACSVerse instrument. A total of $1x10^4$ events were acquired, gated and analyzed using the BD FACS Suite software.

3.2.10 Measurement of mitochondrial respiration

A day prior, a Seahorse XFp Sensor Cartridge was hydrated using Seahorse XF Calibrant overnight at 37°C in a non-CO_2 incubator. The cells used in Seahorse XFp were treated in the same manner as in mitochondrial dynamics flow cytometry experiments. Harvested and centrifuged U937 cells were dissolved in XF Base Medium (pH 7,4), containing 1mM sodium pyruvate, 2mM L-glutamine, 10mM glucose. $2x10^5$ cells in 50µl from each group were seeded into Seahorse XFp Cell Culture miniplates in triplicates. These plates contain 8 wells, therefore only two experimental groups can be analyzed in one assay since two wells are considered as blank according to the manufacturer's protocol. Thus, control and 16 h HDL experimental groups were chosen. Plates were centrifuged at 400xg for 1 min at zero deceleration. Then, 150µl XF Base Medium was added into wells. Cells were incubated in non-CO_2 incubator at 37°C for 45 min. During this incubation, the contents of Seahorse XFp Cell Mito Stress Kit, which are oligomycin (50µM), FCCP (50µM), rotenone/antimycin A (25µM), were prepared according to the manufacturer's instructions. Afterwards, XFp Cell Mito Stress Kit was applied and the plates were analyzed using Agilent Seahorse XFp Analyzer.

3.2.11 Statistical analysis

Western blot results were compared with each other using Kruskal-Wallis test and rest of the samples were compared with each other using two-tailed ratio or paired Student's t-test. GraphPad Prism 8 software was used for statistical analysis and graphical representations. The results were represented as the mean ± SD of at least 3 experimental repeats. P value < 0.05 was considered as statistically significant.

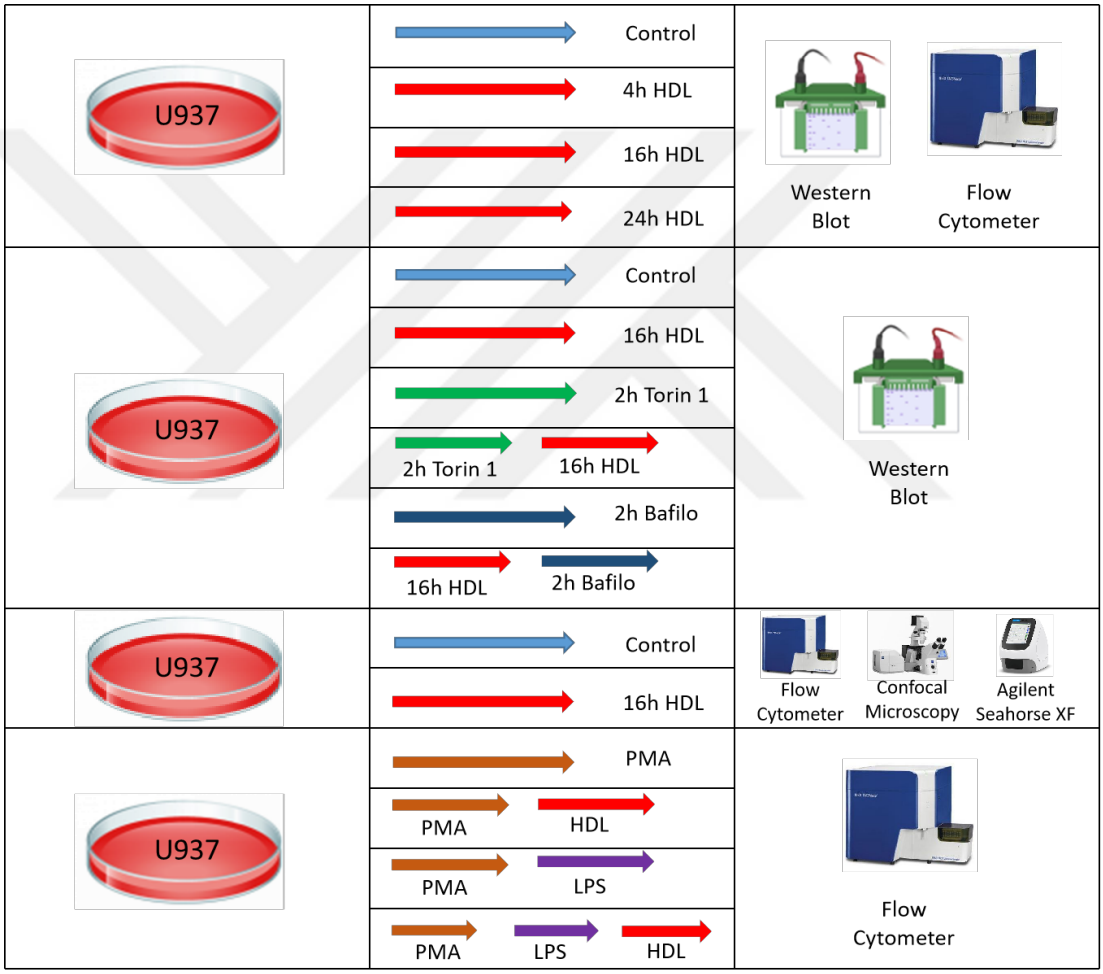

Figure 6. Experimental design.

4 RESULTS

4.1 The Effect of HDL on Cell Viability

U937 human monocyte cell line which is frequently used in atherosclerosis and cholesterol metabolism studies was used in this study (63). In international guidelines, HDL-C levels <40mg/dl in men and <50mg/dl in women are considered low HDL and defined as a cardiovascular risk factor (18). However, in *in vitro* studies, HDL amounts differ from *in vivo* values and are used in the range of 20-100µg/ml (64). The reason for this is that HDL in tissues is perceived in low amounts from blood and forms aggregates when used in physiological amounts. In accordance with this, cells were exposed to 20, 50 and 100µg/ml HDL for 4, 16, and 24 hours, respectively. To determine the effect of HDL on cell viability and toxicity in this cell line, MTT assay was performed at the end of these time periods. It was determined that cell viability of HDL treated cells did not change compared to control cells (Figure 7). We continued using these HDL concentrations since they didn't have any cytotoxic effects on the cells.

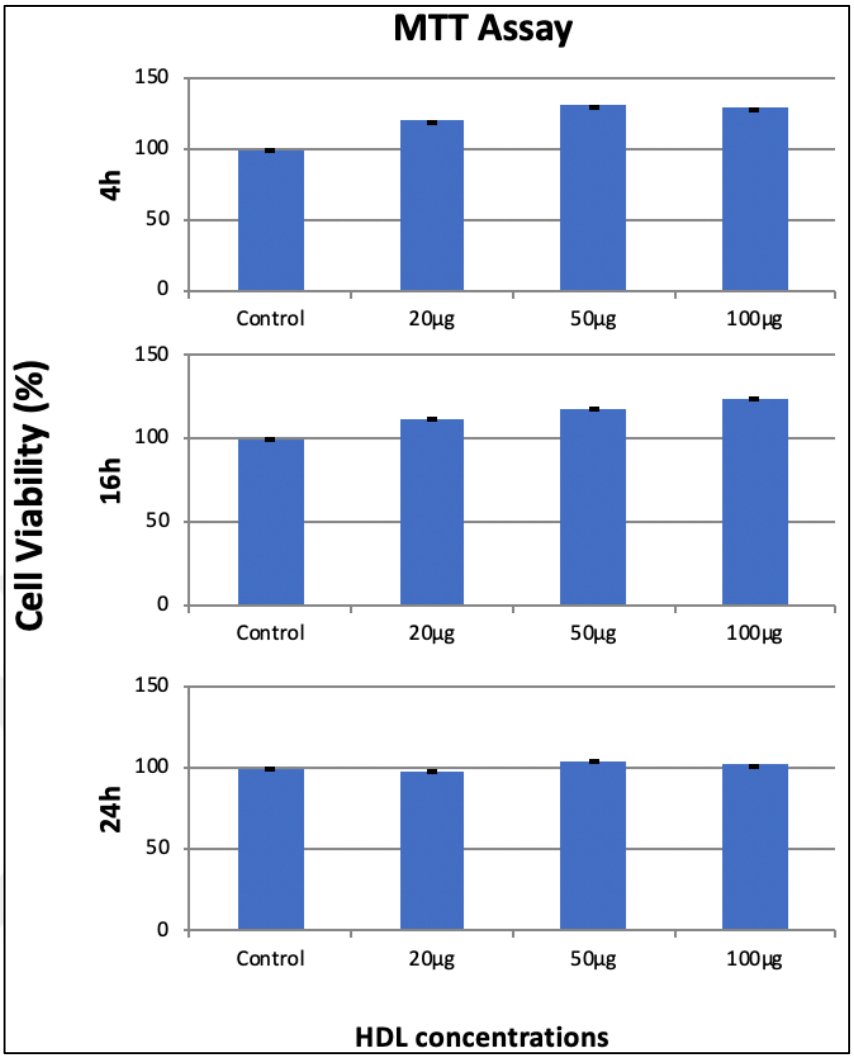

Figure 7. Cytotoxic effect of HDL on U937 cells.

(U937 cells were incubated with different concentrations of HDL from 20µg to 100µg for 4, 16 and 24 h. MTT assay was performed to measure the effect of HDL on cell viability. HDL treated cells were normalized to untreated control cells. The bar graph represents the mean ± SD values of three independent experiments ($p > 0,05$).)

4.2 The Effect of HDL on Autophagy in U937 Cells

4.2.1 Autophagy induction in U937 cells upon HDL treatment

The levels of LC3B-II protein, which is one of the important key markers of autophagy induction (65), was analyzed by western blotting. Cells were incubated with 20 to 100µg/ml of HDL for 4 to 24 hours. It was shown that the LC3B-II protein level was significantly increased in cells treated with 100µg/ml HDL for 16 hours (Figure

8). As a result, we used 100µg/ml HDL for 16 hours in the following experiments. In addition, the same dose was used in autophagic flux experiments in the presence of HDL.

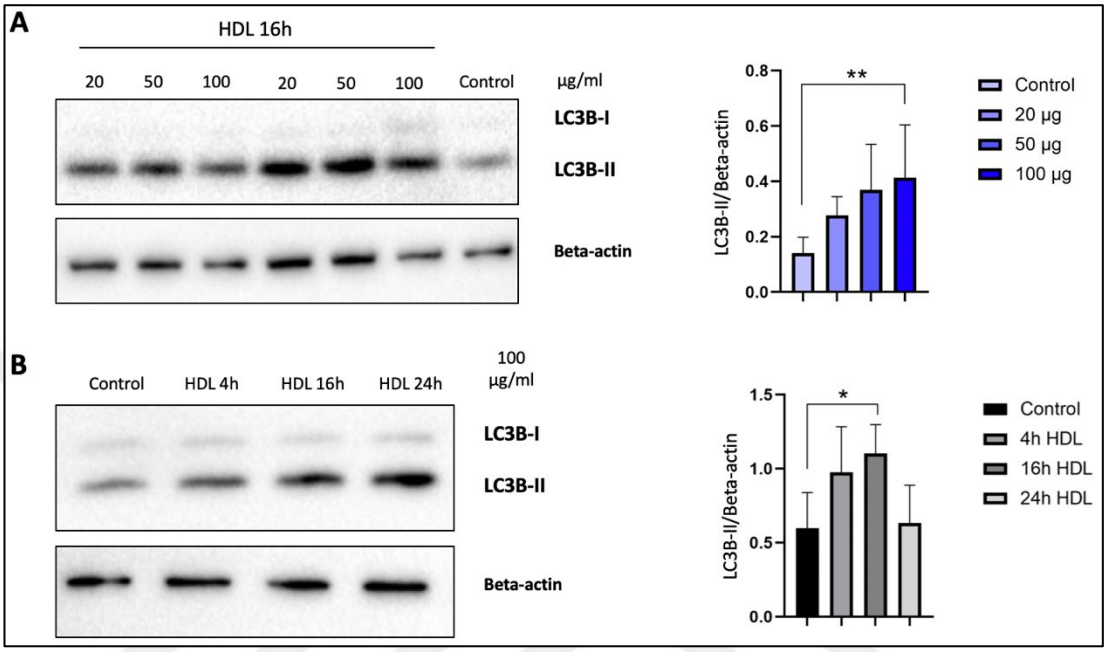

Figure 8. Effects of HDL on LC3B-II levels in U937 cells.

(15% SDS-PAGE gel was used to separate cell lysates after treating cells (A) with 20, 50, 100µg/ml HDL (B) for 4, 16, 24 hours. LC3B-II levels were analyzed by western blotting. Beta-actin is used as an internal control. Protein band density was measured using Image Lab software. Bar graphs show the average of (A) four, (B) five independent experiments. Statistical analysis was performed with the Kruskal-Wallis test. Error bars are given as mean ± SD values. (A) $p<0,01$, (B) $p<0,05$.)

To further analyze the autophagy induction, p62 protein levels were also examined in the presence and the absence of HDL for 4, 16 and 24 h. p62/SQSTM1 acts by binding directly with LC3. p62/SQSTM1 levels were used as a second marker in addition to LC3B to monitor autophagic activity (66). However, HDL treatment did not significantly affect the p62 protein levels (Figure 9).

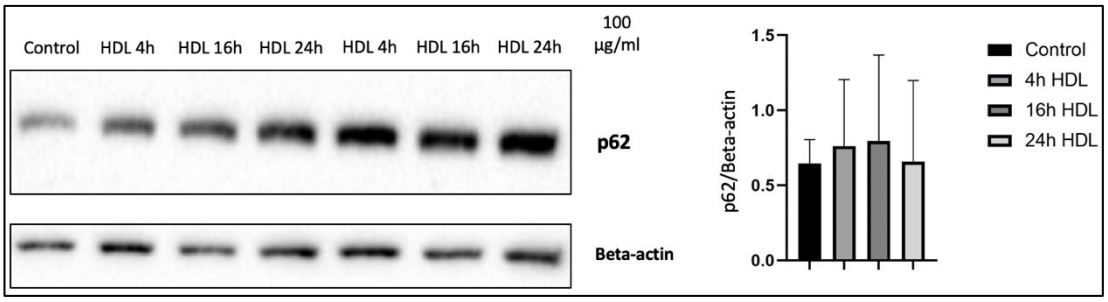

Figure 9. Effects of HDL on p62 levels in U937 cells.

(Cell lysates obtained by treating cells with 100µg/ml HDL for 4, 16, 24 h were run in 12% SDS-PAGE gel. p62 levels were analyzed by western blotting. Beta-actin is used as an internal control. Protein band density was measured using Image Lab software. Bar graphs show the average of three independent experiments. Statistical analysis was performed with the Kruskal-Wallis test. Error bars are given as mean ± SD values. $p>0,05$.)

4.2.2 Autophagic flux in U937 cells upon HDL treatment

Various autophagy activators and inhibitors are used in literature to assess autophagic flux. Autophagy is induced by inhibition of the mTOR pathway in the absence of nutrients in the cell. Torin 1 is a widely used autophagy inhibitor and it inhibits the mTOR complex which is in the initial step of autophagy (67). Bafilomycin as an autophagy inhibitor changes the lysosomal pH and prevents the lysosome from joining with the autophagosome. It leads to the accumulation of autophagic vesicles in the cytoplasm. As a result, an increase in LC3B-II level is observed after bafilomycin treatment. Therefore, bafilomycin is one of the most prominent inhibitors for the monitoring of autophagic flux. (68).

In our study, we observed the highest LC3B-II protein levels at 100nM Torin 1 for 2 h and 25nM bafilomycin for 2 h (data not shown). Therefore, these concentrations were used in further experiments with HDL.

In order to see the effect of HDL on autophagic flux, cells were treated with HDL in the presence and absence of Torin 1 and bafilomycin. In comparison to the control, U937 cells treated with bafilomycin at a concentration of 25nM for two hours had statistically higher levels of LC3B-II. (Figure 10). Although LC3B-II protein levels

increased after HDL treatment, this increase was not significant when HDL treatment was combined with the autophagy modulators.

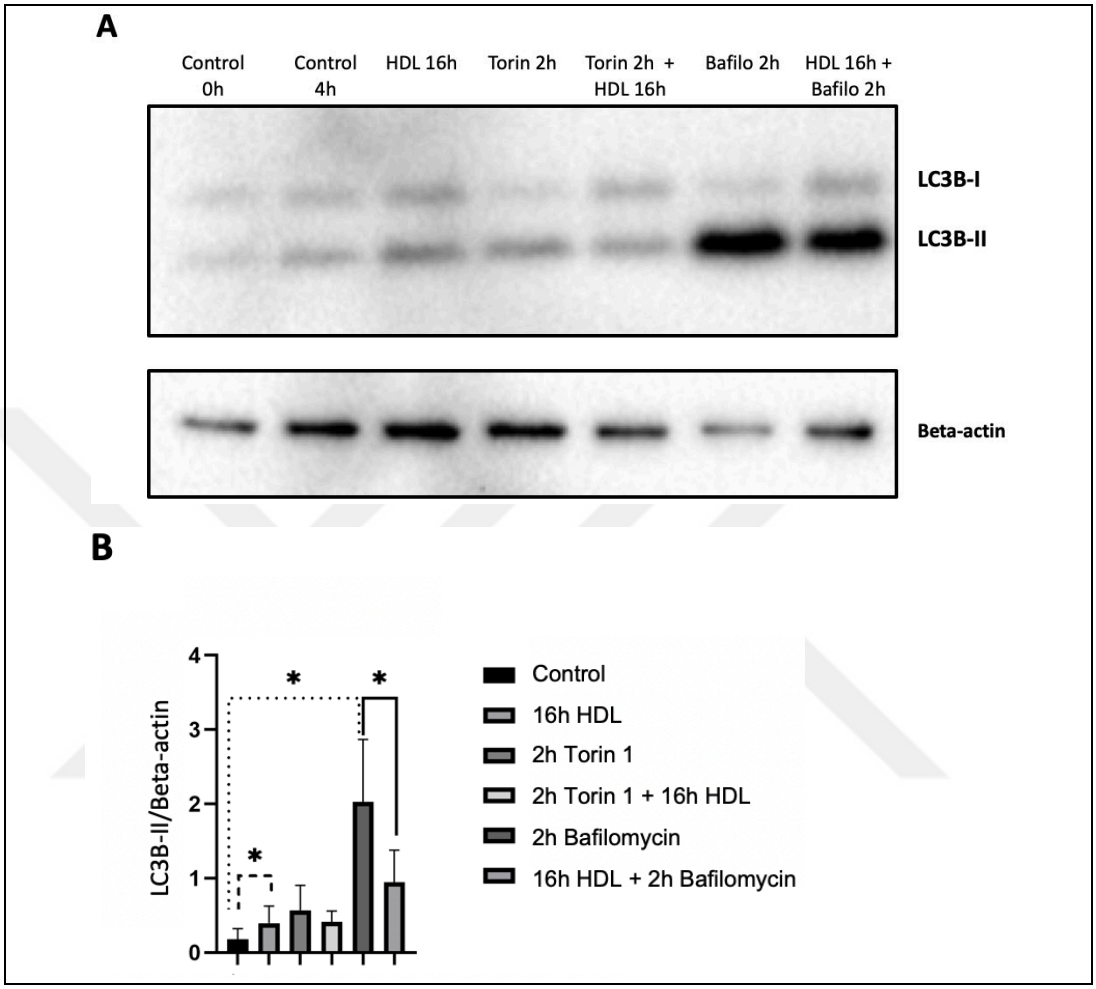

Figure 10. Autophagic flux in U937 cells.

((A) Cells were treated with Torin1 (100nM, 2 h) or bafilomycin (25nM, 2 h) in the presence of HDL (100µg/ml) for 16 h and LC3B-II levels was compared to control (Control 4h) by western blotting. Beta-actin is used as an internal control. Protein band density was measured using Image Lab software. (B) Bar graphs show the average of six independent experiments. Statistical analysis was performed with the Kruskal-Wallis test. Error bars are given as mean ± SD values ($p<0,05$).)

In addition to LC3B, p62/SQSTM1 levels were used as another marker to monitor autophagic flux upon treatment with autophagy modulators. p62 levels were unchanged by the combination of the autophagy activator Torin 1 and the autophagy inhibitor bafilomycin with HDL treatment (Figure 11).

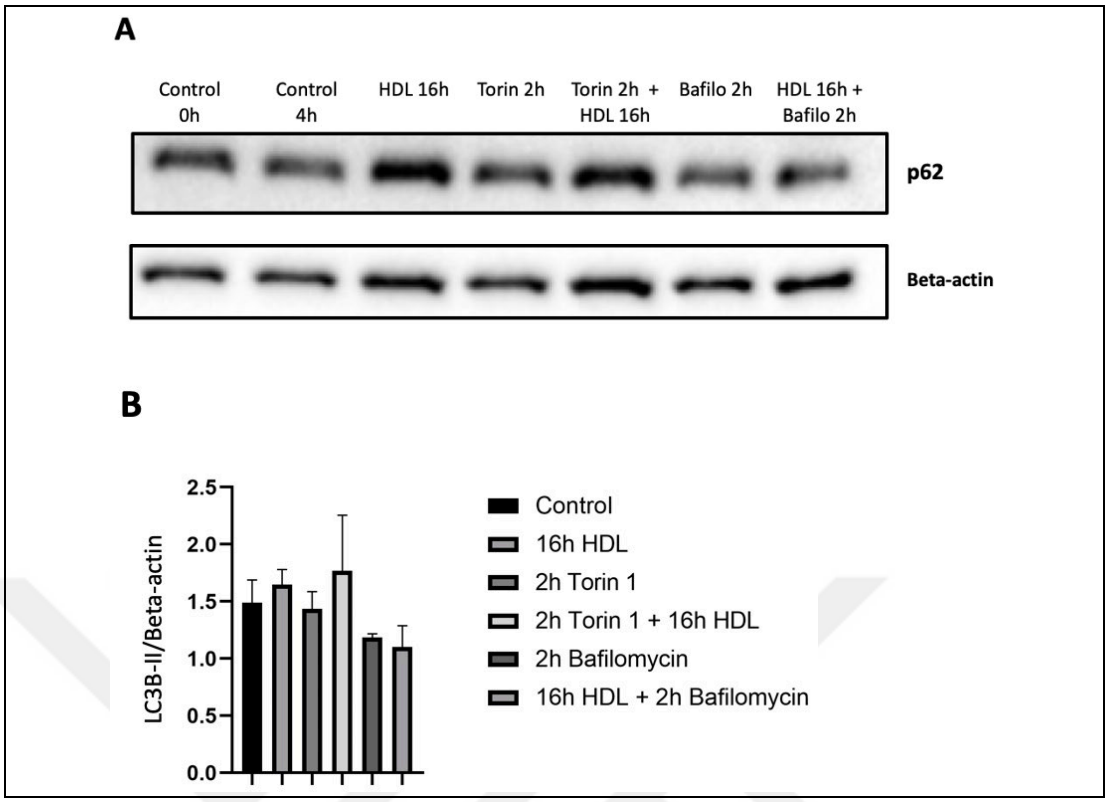

Figure 11. p62 levels in autophagic flux.

((A) Cells were treated with Torin1 (100nM, 2 h) or bafilomycin (25nM, 2 h) in the presence of HDL (100µg/ml) for 16 h and p62 levels was compared to control (Control 4h) by western blotting. Beta-actin is used as an internal control. Protein band density was measured using Image Lab software. (B) Bar graphs show the average of two independent experiments. Statistical analysis was performed with the Kruskal-Wallis test. Error bars are given as mean ± SD values ($p>0,05$).)

4.2.3 Expression of LC3B in HDL treated U937 cells by confocal microscopy

In addition to western blot analysis, LC3B levels were also analyzed by immunofluorescence. LC3B puncta formation was observed under confocal microscopy. Cells were treated with 100µg/ml HDL for 16 hours. Since the nuclei of U937 are quite large, LC3B puncta formation couldn't be adequately observed and puncta count couldn't be performed successfully. However, consistent with our western blot results, an increase was observed in LC3B immunostaining after 16 h of HDL treatment compared to the control group (Figure 12).

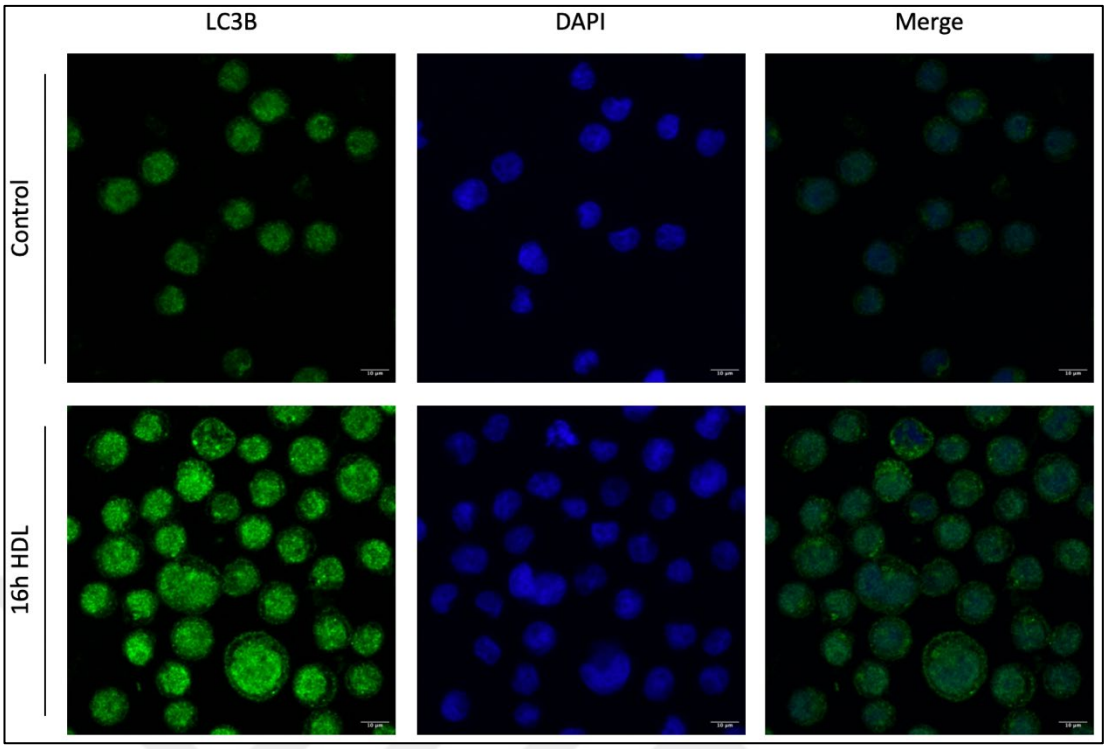

Figure 12. LC3B immunostaining in HDL treated U937 cells.

(The cells were incubated with 100µg/ml HDL for 16 h. Cells were fixed, probed with LC3B and stained with Alexa fluor-488 conjugated secondary antibody. NucBlue was used for nucleus staining. Images were taken with 40x objective using Zeiss LSM 700 confocal microscope. Images are representatives of three independent experiments.)

4.3 The Effect of HDL on Mitochondrial Dynamics in U937 Cells

4.3.1 Cell size and granularity variation in HDL treated U937 cells

Variations in cell diameter measured by forward scatter (FSC) and granularity measured by side scatter (SSC) were observed by flow cytometry in U937 cells incubated with HDL at different time periods. As a result, U937 cells incubated with 100µg/ml HDL for 4, 16 and 24 hours showed a significant increase in SSC values from the fourth hour compared to the control, due to HDL treatment. The highest increase was observed at 16 h (Figure 13). SSC provides information about the granular contents and internal complexity of the cells. SSC is helpful in identifying cells with variable structures such as monocytes and granulocytes.

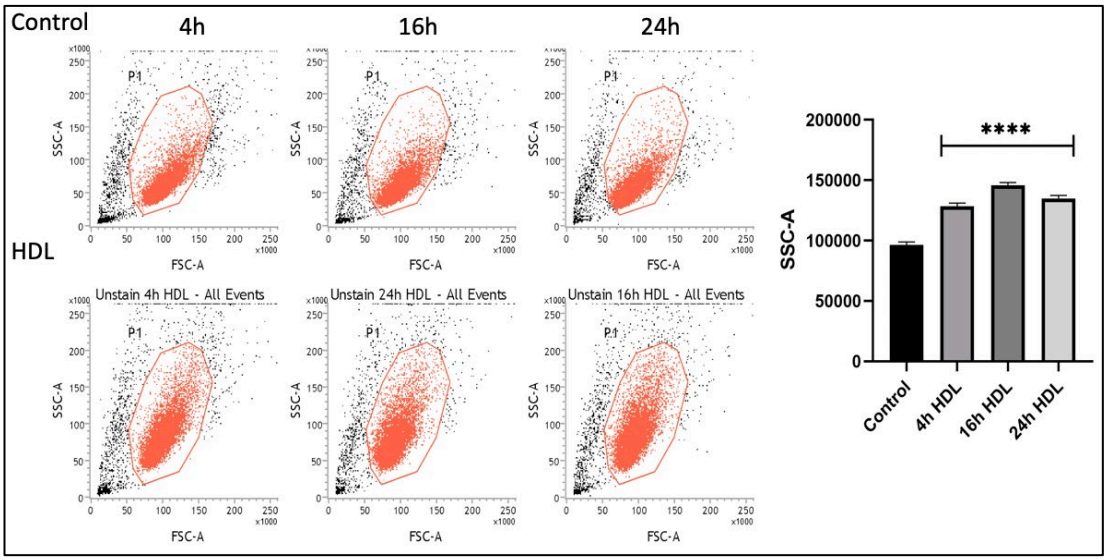

Figure 13. Size and granularity changes in HDL treated U937 cells.

(The cells were incubated with 100µg/ml HDL for 4, 16, and 24 h. Side scatter (SSC) values were measured by flow cytometry and analyzed using BD FACS Suite software. Bar graphs show the average of six independent experiments. Statistical analysis was performed with Student's t test. Error bars are given as mean ± SD values ($p<0,001$).)

4.3.2 Changes in mitochondrial dynamics in HDL treated U937 cells

Mitochondrial dynamics constitute as a crucial factor of mitochondria's health, leading us to know more about cellular homeostasis and function. Mitochondrial dysfunction and ROS lead to the development of various disorders, including cardiovascular diseases (6). We monitored alterations in mitochondrial dynamics in U937 cells, since monocytes and macrophages play a crucial role in the early stages of atherosclerosis progression.

In order to monitor the changes in mitochondrial functions, U937 cells were incubated with 100µg/ml HDL at for 4, 16, and 24 hours. The cells were stained with mitochondria specific fluorescent dyes. Mitochondrial membrane potential (MMP), mitochondrial superoxide and mitochondrial mass were measured by flow cytometry. As a result, a significant decrease was observed in MitoTracker Green FM (mitochondrial mass) and MitoTracker Red CMXRos (MMP) staining upon 16 h of

HDL treatment. HDL treatment did not significantly change MitoSOX levels (Figure 14).

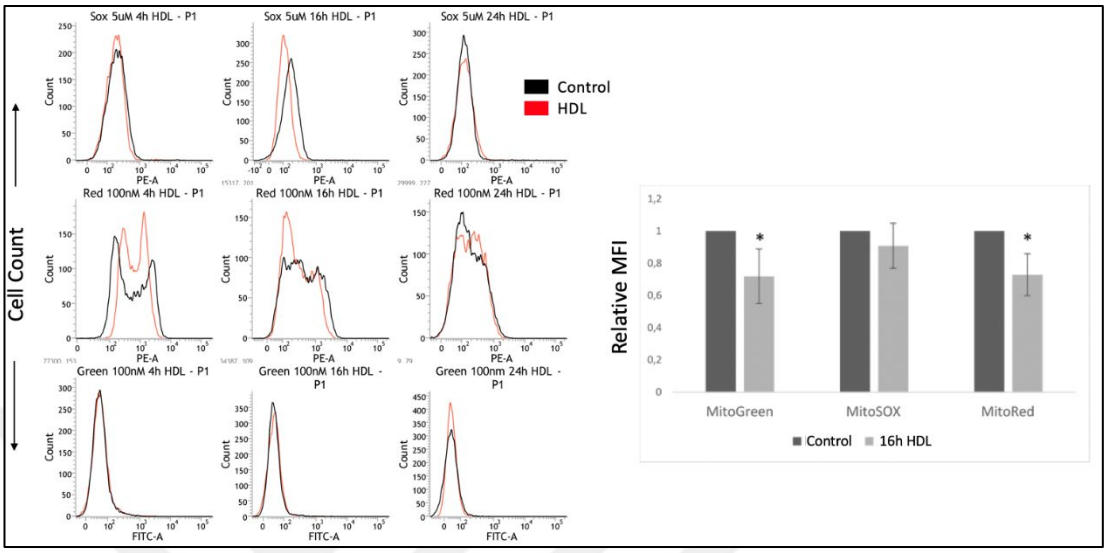

Figure 14. The effect of HDL on mitochondrial dynamics by flow cytometry.

(The cells were incubated with 100µg/ml HDL for 4, 16 and 24 h and stained with 5µM MitoSOX, 100nM MitoTracker Red CMXRos and 100nM MitoTracker Green FM. Mean fluorescence intensity (MFI) was measured by flow cytometry and analyzed using BD FACS Suite software. Bar graphs show the average of four independent experiments. Results were normalized to control group. Statistical analysis was performed with Student's t test. Error bars are given as mean ± SD values ($p<0,05$).)

4.3.3 Changes in mitochondrial dynamics in HDL treated U937 cells by confocal microscopy

Confocal microscopy imaging was performed to verify the results obtained from flow cytometry. To this extent, U937 cells were incubated with 100µg/ml HDL for 16 h and were probed with 5µM MitoSOX, 50nM MitoTracker Red CMXRos and 100nM MitoTracker Green FM. Consistent with our flow cytometry results, a decrease was observed in MitoGreen and MitoRed levels when control and HDL treated samples were compared. We did not observe any changes in MitoSOX levels (Figure 15).

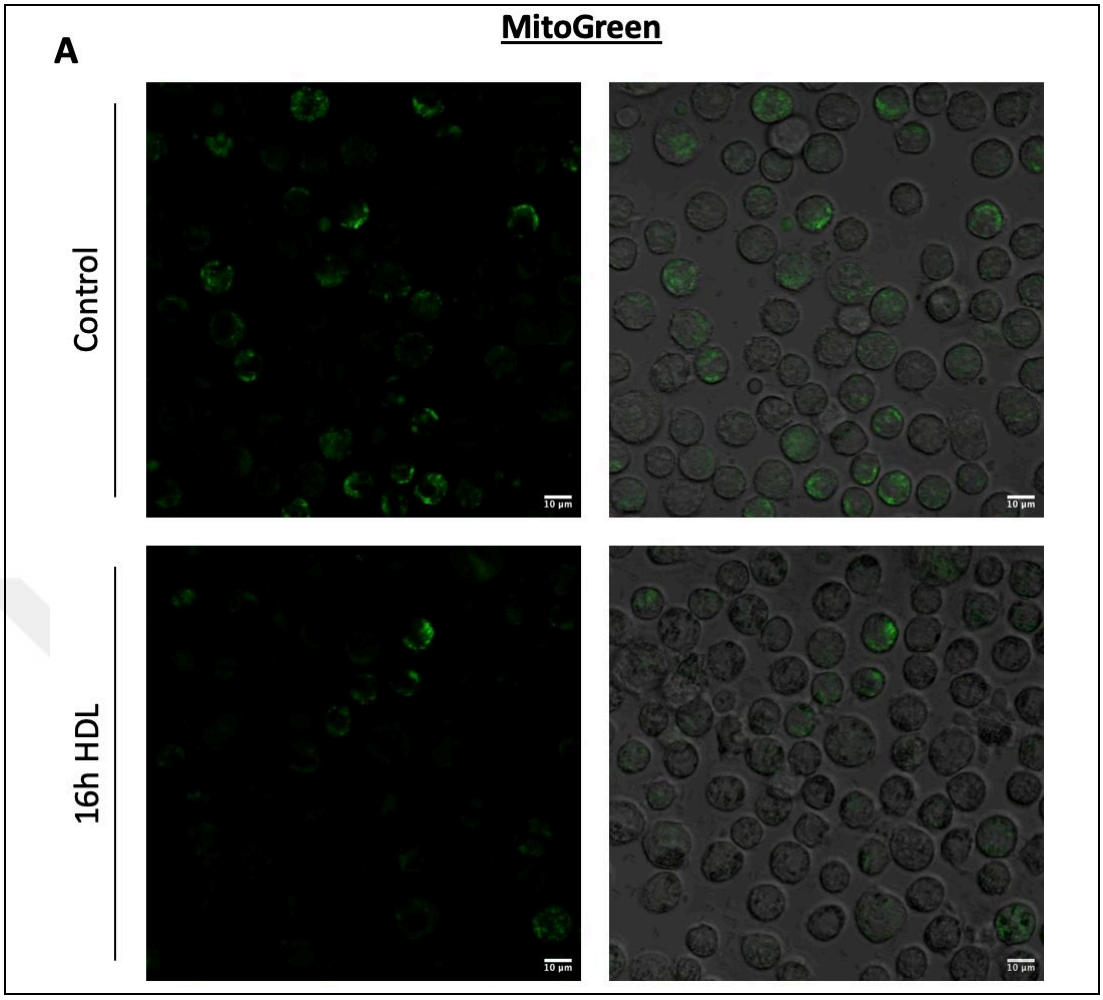

Figure 15. The effect of HDL on mitochondrial dynamics by confocal microscopy.

(The cells were incubated with 100µg/ml HDL for 16 h and stained with (A) 100nM MitoTracker Green FM, (B) 5µM MitoSOX and (C) 50nM MitoTracker Red CMXRos. Images were taken with 40x objective using Zeiss LSM 700 confocal microscope. Corrected total cell fluorescence (CTCF) was measured using ImageJ software. (D) Bar graphs show the CTCF of 50 cells from each group. Statistical analysis was performed with Student's t test. Error bars are given as mean ± SD values ($p<0,05$).)

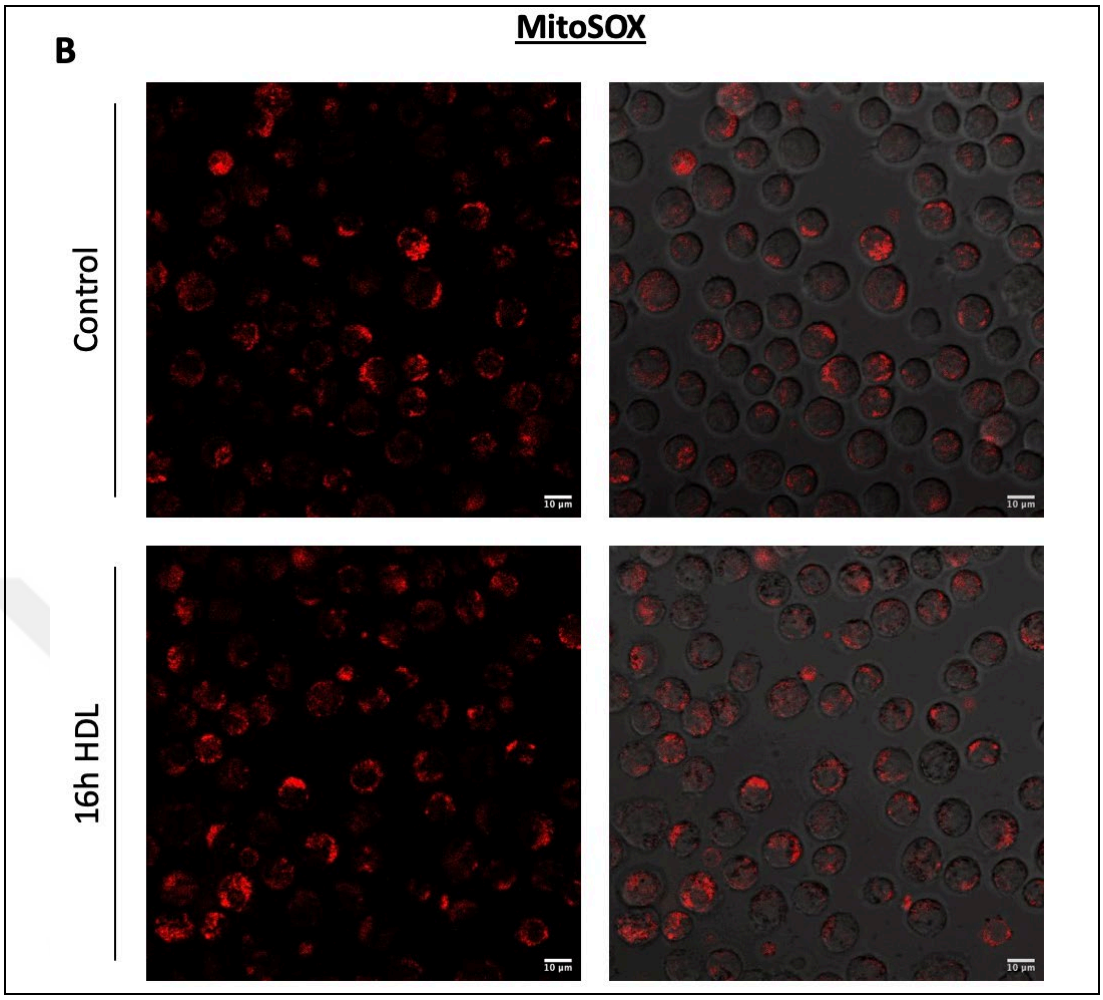

Figure 15. The effect of HDL on mitochondrial dynamics by confocal microscopy (continued).

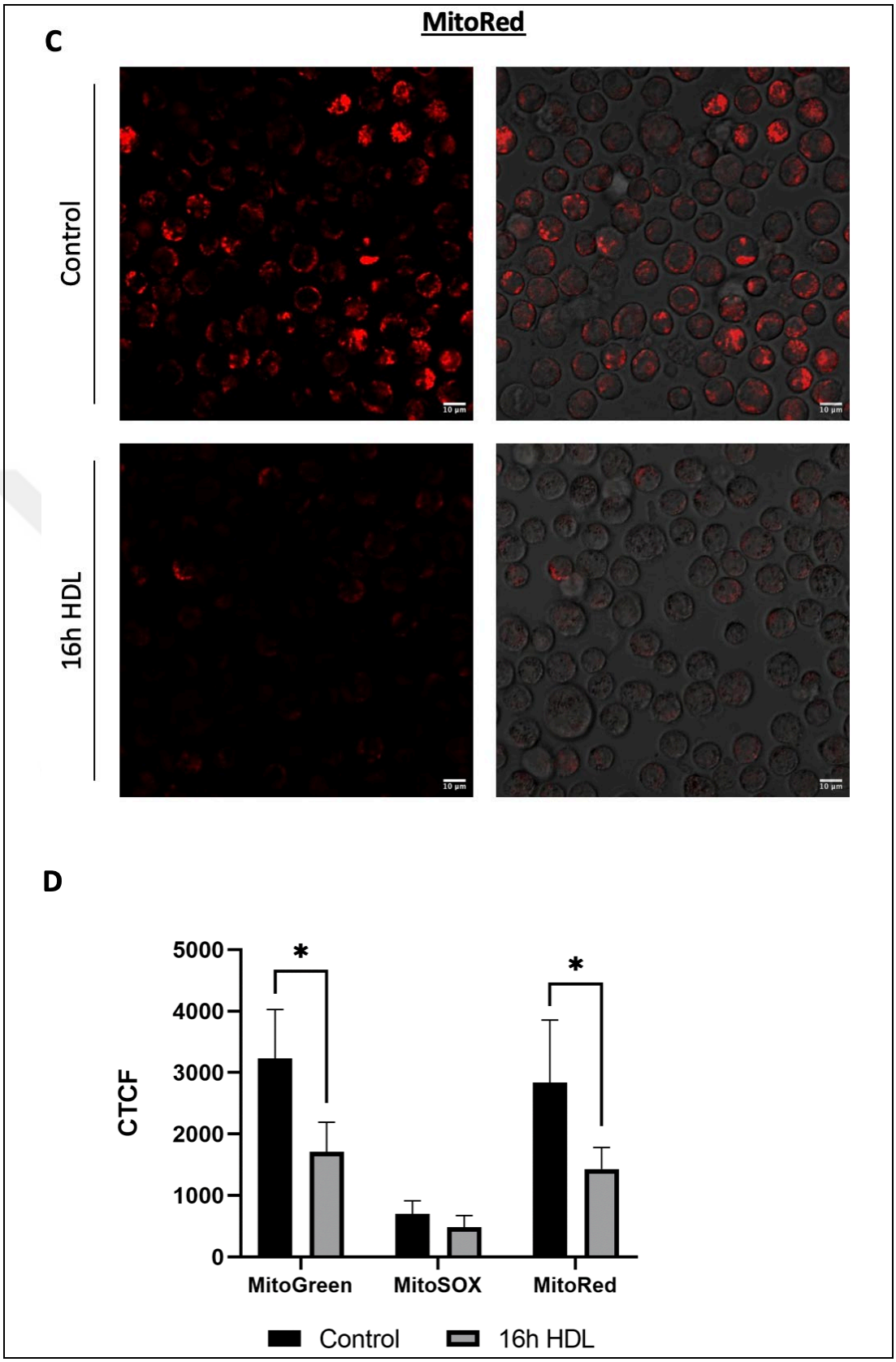

Figure 15. The effect of HDL on mitochondrial dynamics by confocal microscopy (continued).

4.3.4 Mitochondrial respiration analysis for HDL treated U937 cells

In addition to flow cytometry and confocal microscopy analysis, we examined the mitochondrial respiration using XFp Cell Mito Stress Kit for Agilent Seahorse XFp analyzer. U937 cells were incubated with 100µg/ml HDL for 16 h. Samples were prepared according to the manufacturer's protocol. Oligomycin, FCCP and rotenone/antimycin A mixture were used as ETC comlex V inhibitor, uncoupler and ETC complex I and III inhibitor respectively. According to these experiments, cells treated with 100µg/ml HDL had decreased mitochondrial respiration rates compared to the control group. Maximal respiration and ATP production rates of HDL treated group were also lower than the control group (Figure 16).

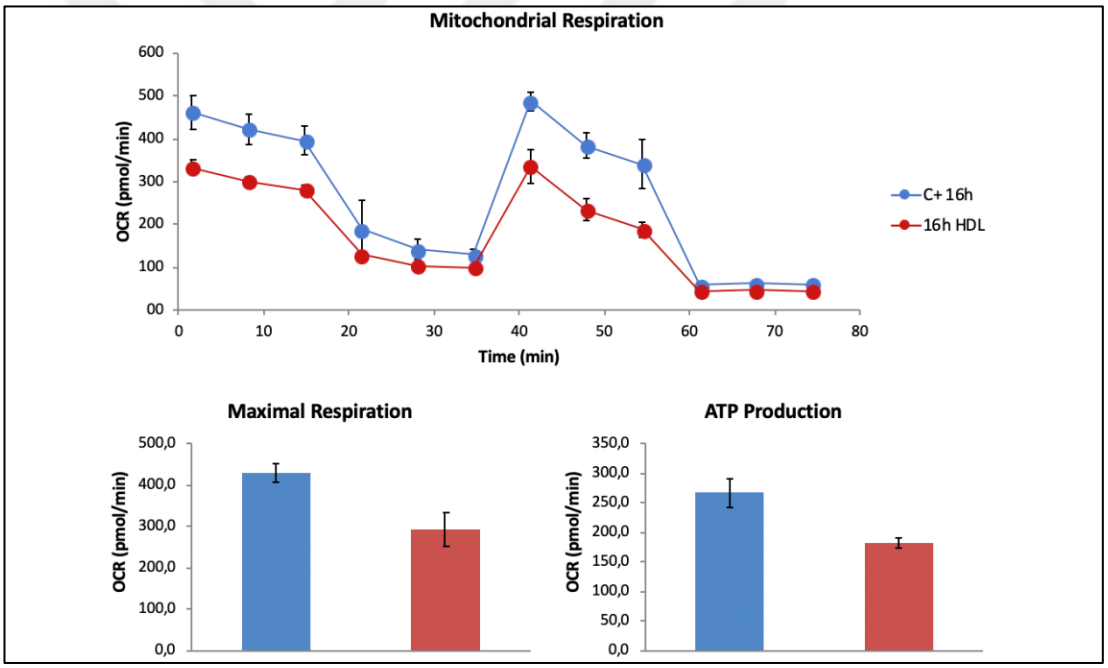

Figure 16. Mitochondrial respiration and ATP production rates for HDL treated U937 cells.

(The cells were incubated with 100µg/ml HDL for 16 h. XFp Cell Mito Stress Kit was used for mitochondrial respiration analysis by Agilent Seahorse XFp Analyzer according to the manufacturer's protocol. Bar graphs show the average of three independent experiments. Error bars are given as mean ± SD values obtained by three consecutive readings of each sample at each step.)

4.3.5 Determination of M1 and M2 macrophage differentiation (polarization) in HDL treated U937 cells

The changes that we observed in cell granularity with SSC (Figure 13) lead us to think that HDL could be modulating monocytes' internal complexity and may be causing them to differentiate. We further investigated the effect of HDL in U937 cells by performing cell surface marker analysis for macrophage polarization. We used CD64 and CD86 surface markers for M1 pro-inflammatory phenotype and CD163 and CD206 surface markers for M2 anti-inflammatory phenotype macrophages. As a result, U937 cells incubated with 100µg/ml HDL for 16 h showed a significant increase in CD86 surface marker and a significant decrease in CD163 surface marker compared to the control. No HDL related changes were observed in CD11c, CD64 and CD206 markers (Figure 17).

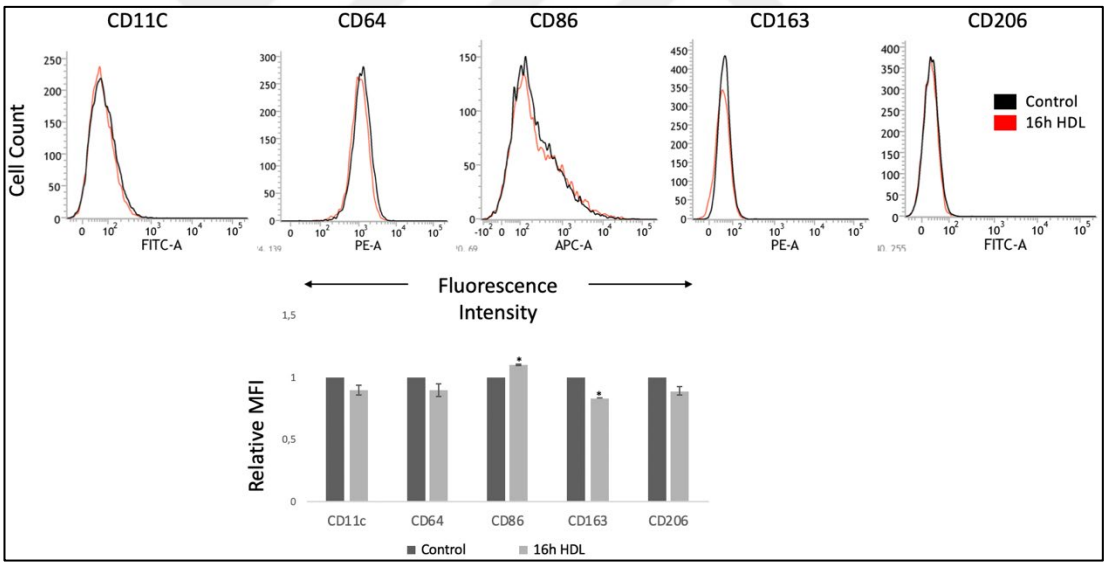

Figure 17. The effect of HDL on M1 and M2 phenotype surface markers by flow cytometry.

(The cells were incubated with 100µg/ml HDL for 16 h and the mean fluorescence intensity (MFI) was measured by flow cytometry and analyzed using BD FACS Suite software. Staining was performed with CD11c for macrophage phenotype, CD64 and CD86 for M1 phenotype, CD163 and CD206 for M2 phenotype. Bar graphs show the average of two independent experiments. Results were normalized to control group. Statistical analysis was performed with Student's t test. Error bars are given as mean ± SD values (CD 86 $p<0,05$, CD163 $p<0,05$).)

4.3.6 Determination of M1 and M2 macrophage differentiation (polarization) in PMA-differentiated U937 cells

When U937 monocytic cells are treated with phorbol myristate acetate (PMA), they differentiate into macrophage cells (69). After HDL treatment, U937 cells with monocytic phenotype did not show the expected change in the expression of surface markers. Thus, for further investigation, we analyzed whether there was a change in these surface markers in differentiated cells. For this purpose, U937 cells were first differentiated into macrophage cells in the presence of PMA, and the effect of HDL was examined. Lipopolysaccharide (LPS) was used for M1 phenotype polarization.

In order to determine the optimal dose and incubation time for PMA, U937 cells were incubated with 40nM and 100nM PMA for 24, 48 and 72 h. Upon differentiation, suspension U937 cells become adherent and start to attach to the bottom of the culture plate. They also acquire a macrophage-like phenotype. We determined that 40nM PMA for 48 h was efficient to differentiate U937 cells while not affecting cell viability (data not shown).

First, U937 cells were differentiated into macrophages with 40nM PMA for 48 h. After 24 h treatment with 100µg/ml HDL in differentiated cells, we observed a significant increase for macrophage phenotype marker CD11c and M2 phenotype markers CD163 and CD206. M1 phenotype marker CD86 was found to be significantly increased in the presence of PMA + HDL and PMA + LPS + HDL compared to control. For the M2 phenotype marker CD163 and CD206, a significant decrease was observed in PMA + HDL + LPS compared to PMA + HDL. No difference was seen after PMA, LPS and HDL treatment for CD64 (Figure 18).

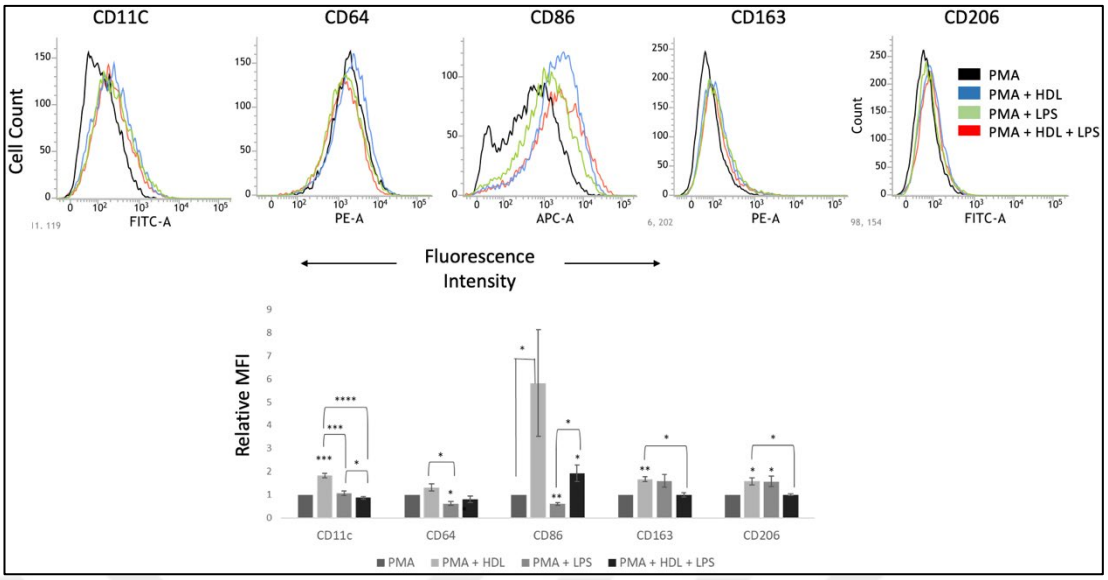

Figure 18. The effect of LPS and HDL on M1 and M2 phenotype surface markers in PMA-differentiated U937 cells by flow cytometry.

(After the cells have differentiated into macrophages by 40nM PMA incubation for 48 h, they were incubated for 24 h with 100ng/ml LPS and 100µg/ml HDL. Mean fluorescence intensity (MFI) was measured by flow cytometry and analyzed using BD FACS Suite software. Staining was performed with CD11c for macrophage phenotype, CD64 and CD86 for M1 phenotype, CD163 and CD206 for M2 phenotype. Bar graphs show the average of three independent experiments. Results were normalized to the PMA only control group. Statistical analysis was performed with Student's t test. Error bars are given as mean ± SD values (* $p<0,05$; ** $p<0,01$; *** $p<0,005$; **** $p<0,001$).)

5 DISCUSSION

High Density Lipoprotein (HDL) is primarily responsible for removing cholesterol from the blood and controlling RCT to the liver, but current findings have revealed that it also possesses anti-apoptotic, anti-inflammatory and cardiovascular protective properties (18). However, how HDL-C levels contribute to HDL's function is still being studied. There are studies stating that there is a connection between HDL and autophagy, which plays an important role in cell homeostasis, and inherited metabolic diseases (16,70). One of these metabolic pathways is the link between lipid metabolism and autophagy. The connection between autophagy and cholesterol metabolism, especially HDL, is still unknown and open to research. In our study, the expression of proteins that play a key role in autophagy and autophagic flux were investigated at different time points in the presence and absence of HDL. At the same time, the effect of HDL on mitochondrial dynamics and the differentiation of monocytes were analyzed in the U937 monocytic cell line. Monocytic cell line was chosen because they play a key role in the development and progression of atherosclerosis, cholesterol transport and is a site of action for HDL (56).

Autophagy functions as a survival mechanism for the cell. Considering the anti-inflammatory, cholesterol-scavenging and endothelial protective functions of HDL, it is very likely for HDL to intersect with autophagic pathways. In cholesterol transport, autophagy leads to the degradation of ApoB aggregates to greatly limit the secretion of dysfunctional LDL (37). Increasing autophagic activity to assist lipid breakdown in insulin-resistant obese individuals may contribute to increase HDL's function as well (38). In addition, free fatty acids stimulate autophagy, indicating that autophagy acts as a defense mechanism to prevent intracellular lipid accumulation.

There are several studies showing that cellular cholesterol modifications are important in autophagy regulation. Decreased cholesterol stimulates autophagy in many cell types by inhibiting mTOR complex, which is related to cell growth and metabolic processes (71). Conversely, hypercholesterolemia suppresses autophagy by activating mTOR signaling. The effect of the presence and different doses of HDL on

autophagy in monocytes were reported for the first time in this study. According to HDL values in the range of 20-100μg/ml used in *in vitro* studies, 100μg/ml used in our study corresponds to a physiologically high HDL level (HDL-C >60mg/dl) in humans (64,72). We found that 100μg/ml HDL increases autophagy in U937 cells. Although this can be interpreted as an increase in autophagic activity in parallel with the amount of HDL in individuals with high HDL-C levels, it needs to be confirmed in *in vivo* studies. In accordance with these results, Gerster and her colleagues demonstrated that in similar concentrations at 18 h, HDL induced an increase in conjugation of LC3-II during autophagy. Thus, NF-kappa B activation and induction of cytokine expression were prevented in T84 human intestinal epithelial cell line (73). Together, these results provide an initial evidence that HDL may control inflammation through autophagy.

Muller and his colleagues showed that in human microvascular endothelial cells, HDLs prevent the oxLDL-induced activation of the ER stress and inhibited autophagy. They used HDL for 8 h, and as a result, no increase in LC3-II levels was observed. Likewise, in U937 cells, cells were treated with HDL for only 1 hour, and no difference was observed in LC3-II levels compared to the control (42). Different from this article, we demonstrated the effect of HDL on autophagy at different doses and time periods, and reported the changes in autophagic flux. Autophagic flux refers to the rate at which cargo is transported through autophagy to the autophagosome and degraded in the lysosome. Measuring the autophagic flux is an indicator of whether the autophagy mechanism is working in the cell. To measure this, either autophagy inducing agents such as Torin 1 or lysosome inhibitors such as bafilomycin are used. When the effect of HDL in the presence of autophagy activators or inhibitors is examined in U937 cells, we observed that HDL induces autophagic flux, but when compared to the groups where inhibitors and activators are used alone, the autophagic flux is high in these cells at basal level.

It has been reported that the p62/SQSTM1 protein binds to the ubiquitinated cargo and LC3B in the cell during the autophagy process and plays a role in the transport of this structure to the autophagic vesicle. p62 is also thought to be a link between autophagy and ubiquitination, which is an effective process in clearing large protein

aggregates accumulated in the cell. This protein is degraded during autophagy. The reduced levels of p62 in western blot analysis is associated with autophagy. The p62/SQSTM1 protein is a multifunctional adapter protein and has been reported to be involved in cell differentiation and proliferation (66). Furthermore, it has been shown that the p62 protein also binds to Protein kinase C, which plays a role in signaling, cell proliferation and differentiation (74). In U937 cells, p62 levels increased as a result of differentiation into macrophages upon PMA treatment (75). In our study, we observed that 100µg HDL treatment in U937 cells did not significantly increase the p62 levels with HDL treatment for 16 h. Although there was an increase in LC3B levels upon HDL treatment, this increase was not significant as Torin 1 and bafilomycin pretreatment. All of the aforementioned factors, along with the absence of p62 degradation in U937 cells suggest that HDL-induced autophagy may be effective in a different autophagic pathway such as LC3 associated phagocytosis.

Mitochondria are exposed to high amounts of reactive oxygen production due to their role in energy production. This causes mitochondrial DNA mutation and an increase in the number of damaged mitochondria. It is known that oxidized LDL causes mitochondrial ROS formation with pro-inflammatory lipids and increases mitochondrial membrane permeability (53). Although HDL is known to have anti-oxidative properties, there are not enough studies on its role in protecting mitochondria from damage. On the other hand, considering the effect of LDL, HDL is expected to help maintain mitochondrial membrane potential by reducing oxidative stress. In accordance with our hypothesis, mitochondrial membrane potential was decreased in cells treated with HDL for 16 hours. We observed a slight although not significant decrease in mitochondrial superoxide levels in both flow cytometry and confocal microscopy. Along with MMP, mitochondrial mass was significantly decreased as well. Benischke and her colleagues concluded that activation of mitophagy leads to loss of mitochondrial mass in human corneal endothelial cells (76). The loss of MMP and a decrease in mitochondrial mass indicates that HDL may also lead to activation of mitophagy. Reduced mitochondrial respiration and ATP production after HDL treatment provide additional evidence of HDL's impact on the cell's bioenergetic state and induction of glycolysis pathways. It might also alter mitochondrial dynamics

through induction of mitophagy. HDL may prevent mitochondrial dysfunction by reducing ROS production. Thereby, HDL protects mitochondria from damage by reducing oxidant formation and regulating mitochondrial membrane potential and mitochondrial mass.

In recent publications, the relationship between autophagy and serum amyloid A induced nitric oxide production upon HDL treatment in macrophages has been reported in a dose-dependent manner (77). Also, the link between autophagy and HDL-induced macrophage apoptosis has been published, and a dose-dependent role of HDL has been shown (78). Lee at al. has shown that HDL inhibits the differentiation of macrophages into the M1 phenotype (61). Therefore, while HDL causes cell differentiation of monocytes into macrophages, it may cause autophagy activation in the process. This proves us that HDL has a role in innate immunity as well.

The light reflected from the intracellular granules increases the intensity of the SSC measurement, enabling the differentiation of granulocytes and monocytes. We observed that SSC changed from the fourth hour upon HDL treatment. A significant change in the granularity of the cells as a result of the incubation of U937 cells with HDL suggests that HDL can change the internal structure of monocytes. This may be due to HDL being taken up into the cell or because it changes the cell's phenotype. In addition to the literature mentioned above, our observation suggests that HDL may cause differentiation in monocytes.

It is known that HDL, which functions as a protective mechanism for the cell in the development of atherosclerosis, RCT and innate immunity, has anti-inflammatory and anti-atherogenic effects. We predicted that HDL treated monocytes would cause a decrease in M1 and an increase in M2 phenotype surface markers. Although CD64 and CD206 markers did not change in cells treated with HDL for 16 hours, we observed an increase in CD86 for the M1 phenotype and a decrease in CD163 for the M2 phenotype. Macrophages have more CD163 expression than monocytes (79). Since no change was observed in CD206, another key M2 marker, the decrease in CD163 expression and the increase in CD86 surface suggest that HDL affect macrophage

differentiation. In addition, it may also initiate T cell activation and play an active role in controlling inflammation (80).

Afterwards, we checked the effect of HDL on PMA differentiated U937 cells. The fact that the surface marker CD11c increased significantly on PMA-differentiated cells confirms that macrophage differentiation was successful. 100μg/ml HDL treatment for 24 h induced an increase in both M2 surface markers CD163 and CD206. This reveals that HDL promotes a M2 phenotype in macrophage differentiated monocytes. In addition, when M1 type polarization is induced by LPS, CD163 and CD206 levels significantly decreased in the PMA + HDL + LPS group compared to the PMA + HDL group alone. Sanson et al. showed that HDL increases the expression of anti-inflammatory M2 phenotype genes in mouse primary macrophages upon IL-4 stimulation, supporting our results that HDL works on macrophage polarization (62). Studies in the literature indicate that HDL increases M2 phenotype markers after 5-7 days of HDL incubation in primary cell cultures (61). In our study, we used the U937 monocytic cell line and limited HDL incubation to a maximum of 24 hours. In order to see the long-term effects of HDL, the incubation period can be extended and the expression of related genes in the M1/M2 phenotype polarization can be analyzed by RT-qPCR. HDL also has many subtypes (81). The HDL that we used from Lee Bisolutions includes the total HDL obtained from the serum. Different HDL subtypes and treatments with the Apolipoprotein AI protein, which is the main constituent of HDL, can also be examined which state of HDL directly affects the M1/M2 phenotype.

6 CONCLUSION

Despite the fact that the main function of HDL is to transport free cholesterol to the liver, our data suggest that HDL may also play a beneficial role in the control of inflammation through macrophage polarization. HDL changes the granular structure of monocytes, and also causes changes in M1 and M2 phenotype markers.

The size, density, intracellular accumulation of HDL particles can cause the activation of autophagy, which plays a role in the breakdown of accumulated intracellular protein and lipid aggregates. In our study, the dose that resulted in autophagy activation in U937 cells corresponds to high HDL values in humans. This may cause higher autophagy activity in individuals with higher HDL-C levels. Therefore, supporting the in vitro results with in vivo studies is important to elucidate the link between HDL and autophagy. We will learn more about the functions of HDL by observing how levels of HDL affect the autophagy processes. In addition, HDL has a direct effect on mitochondrial functions and dynamics and it may cause mitophagy activation. Furthermore, decrease in mitochondrial membrane potential and mitochondrial mass indicate that HDL protects mitochondria from damage by causing changes in mitochondrial functions.

7 REFERENCES

1. Jomard A, Osto E. High Density Lipoproteins: Metabolism, Function, and Therapeutic Potential. Vol. 7, Frontiers in Cardiovascular Medicine. Frontiers Media S.A.; 2020.
2. Barter PJ, Nicholls S, Rye KA, Anantharamaiah GM, Navab M, Fogelman AM. Antiinflammatory properties of HDL. Vol. 95, Circulation Research. 2004. p. 764–72.
3. Murphy AJ, Bijl N, Yvan-Charvet L, Welch CB, Bhagwat N, Reheman A, et al. Cholesterol efflux in megakaryocyte progenitors suppresses platelet production and thrombocytosis. Nat Med. 2013;19(5):586–94.
4. Feig JE, Hewing B, Smith JD, Hazen SL, Fisher EA. High-density lipoprotein and atherosclerosis regression: Evidence from preclinical and clinical studies. Vol. 114, Circulation Research. 2014. p. 205–13.
5. Xie Y, Li J, Kang R, Tang D. Interplay Between Lipid Metabolism and Autophagy. Vol. 8, Frontiers in Cell and Developmental Biology. 2020. p. 431.
6. Ploumi C, Daskalaki I, Tavernarakis N. Mitochondrial biogenesis and clearance: a balancing act. FEBS J. 2017 Jan 11;284(2):183–95.
7. Mehta MM, Weinberg SE, Chandel NS. Mitochondrial control of immunity: Beyond ATP. Nat Rev Immunol. 2017;17(10):608–20.
8. Yvan-Charvet L, Wang N, Tall AR. Role of HDL, ABCA1, and ABCG1 transporters in cholesterol efflux and immune responses. Vol. 30, Arteriosclerosis, Thrombosis, and Vascular Biology. 2010. p. 139–43.
9. Zannis VI, Chroni A, Krieger M. Role of apoA-I, ABCA1, LCAT, and SR-BI in the biogenesis of HDL. Vol. 84, Journal of Molecular Medicine. 2006. p. 276–94.
10. Fitzgerald ML, Mujawar Z, Tamehiro N. ABC transporters, atherosclerosis and inflammation. Vol. 211, Atherosclerosis. 2010. p. 361–70.
11. Säemann MD, Poglitsch M, Kopecky C, Haidinger M, Hörl WH, Weichhart T. The versatility of HDL: A crucial anti-inflammatory regulator. Vol. 40, European Journal of Clinical Investigation. John Wiley & Sons, Ltd; 2010. p. 1131–43.
12. Schaefer EJ, Anthanont P, Asztalos BF. High-density lipoprotein metabolism, composition, function, and deficiency. Vol. 25, Current Opinion in Lipidology. 2014. p. 194–9.
13. Linton MF, Yancey PG, Davies SS, Jerome WG, Linton EF, Song WL, et al. The Role of Lipids and Lipoproteins in Atherosclerosis. Science (80-). 2019 Jan 3;111(2877):166–86.
14. Vaisar T. Proteomics Investigations of HDL: Challenges and Promise. Curr Vasc Pharmacol. 2012;10(4):410–21.
15. Gordon SM, Hofmann S, Askew DS, Davidson WS. High density lipoprotein: It's not just about lipid transport anymore. Vol. 22, Trends in Endocrinology and Metabolism. 2011. p. 9–15.

16. deGoma EM, DeGoma RL, Rader DJ. Beyond High-Density Lipoprotein Cholesterol Levels. Evaluating High-Density Lipoprotein Function as Influenced by Novel Therapeutic Approaches. Vol. 51, Journal of the American College of Cardiology. 2008. p. 2199–211.
17. Nofer JR, Kehrel B, Fobker M, Levkau B, Assmann G, Eckardstein A Von. HDL and arteriosclerosis: Beyond reverse cholesterol transport. Vol. 161, Atherosclerosis. Elsevier; 2002. p. 1–16.
18. Frolkis JP, Pearce GL, Sprecher DL. Implications of 2001 cholesterol treatment guidelines based on a retrospective analysis of a high-risk patient cohort. Am J Cardiol. 2002 Mar 15;89(6):765–6.
19. Ballantyness D, Clark RS, Ballantyne FC. The effect of physical training on plasma lipids and lipoproteins. Vol. 4, Clinical Cardiology. 1981. p. 1–4.
20. Chiesa G, Sirtori CR. Apolipoprotein A-IMilano: Current perspectives. Vol. 14, Current Opinion in Lipidology. 2003. p. 159–63.
21. Rodríguez Esparragón F, Hernández Trujillo Y, Macías Reyes A, Hernández Ortega E, Medina A, Rodríguez Pérez JC. Concerning the Significance of Paraoxonase-1 and SR-B1 Genes in Atherosclerosis. Rev Española Cardiol (English Ed. 2006 Feb 1;59(2):154–64.
22. Takaeko Y, Matsui S, Kajikawa M, Maruhashi T, Kishimoto S, Hashimoto H, et al. Association of extremely high levels of high-density lipoprotein cholesterol with endothelial dysfunction in men. J Clin Lipidol. 2019 Jul 1;13(4):664-672.e1.
23. Jakob P, Lüscher TF. Dysfunctional HDL and inflammation: A noxious liaison in adolescents with type 1 diabetes. Vol. 40, European Heart Journal. 2019. p. 3567–70.
24. Duffy D, Rader DJ. Update on strategies to increase hdl quantity and function. Vol. 6, Nature Reviews Cardiology. 2009. p. 455–63.
25. Yang Z, Klionsky DJ. Mammalian autophagy: Core molecular machinery and signaling regulation. Vol. 22, Current Opinion in Cell Biology. NIH Public Access; 2010. p. 124–31.
26. Shintani T, Klionsky DJ. Autophagy in health and disease: A double-edged sword. Vol. 306, Science. NIH Public Access; 2004. p. 990–5.
27. Jin Y, Hong Y, Park CY, Hong Y. Molecular interactions of autophagy with the immune system and cancer. Vol. 18, International Journal of Molecular Sciences. 2017.
28. Yu L, Alva A, Su H, Dutt P, Freundt E, Welsh S, et al. Regulation of an ATG7-beclin 1 program of autophaglic cell death by caspase-8. Science (80-). 2004 Jun 4;304(5676):1500–2.
29. Shimizu S, Kanaseki T, Mizushima N, Mizuta T, Arakawa-Kobayashi S, Thompson CB, et al. Role of Bcl-2 family proteins in a non-apoptopic programmed cell death dependent on autophagy genes. Nat Cell Biol. 2004 Nov 21;6(12):1221–8.
30. Feng Y, He D, Yao Z, Klionsky DJ. The machinery of macroautophagy. Vol. 24, Cell Research. Nature Publishing Group; 2014. p. 24–41.
31. Sugawara K, Suzuki NN, Fujioka Y, Mizushima N, Ohsumi Y, Inagaki F. The crystal structure of microtubule-associated protein light chain 3, a mammalian homologue of Saccharomyces cerevisiae Atg8. Genes to Cells. 2004;9(7):611–8.

32. Pankiv S, Clausen TH, Lamark T, Brech A, Bruun JA, Outzen H, et al. p62/SQSTM1 binds directly to Atg8/LC3 to facilitate degradation of ubiquitinated protein aggregates by autophagy*[S]. J Biol Chem. 2007 Aug 17;282(33):24131–45.
33. Yu L, Chen Y, Tooze SA. Autophagy pathway: Cellular and molecular mechanisms. Vol. 14, Autophagy. 2018. p. 207–15.
34. Singh R, Kaushik S, Wang Y, Xiang Y, Novak I, Komatsu M, et al. Autophagy regulates lipid metabolism. Nature. 2009;458(7242):1131–5.
35. Ouimet M, Franklin V, Mak E, Liao X, Tabas I, Marcel YL. Autophagy regulates cholesterol efflux from macrophage foam cells via lysosomal acid lipase. Cell Metab. 2011 Jun 8;13(6):655–67.
36. Zhang X, Evans TD, Jeong SJ, Razani B. Classical and alternative roles for autophagy in lipid metabolism. Vol. 29, Current Opinion in Lipidology. NIH Public Access; 2018. p. 203–11.
37. Pan M, Maitin V, Parathath S, Andreo U, Lin SX, St. Germain C, et al. Presecretory oxidation, aggregation, and autophagic destruction of apoprotein-B: A pathway for late-stage quality control. Proc Natl Acad Sci U S A. 2008;105(15):5862–7.
38. Kovsan J, Blüher M, Tarnovscki T, Klöting N, Kirshtein B, Madar L, et al. Altered autophagy in human adipose tissues in obesity. J Clin Endocrinol Metab. 2011;96(2):96.
39. Davidson MH, Pulipati VP. Overview of Lipid Metabolism - Endocrine and Metabolic Disorders - MSD Manual Professional Edition [Internet]. 2021 [cited 2022 Aug 10]. Available from: https://www.msdmanuals.com/professional/endocrine-and-metabolic-disorders/lipid-disorders/overview-of-lipid-metabolism
40. Davidson MH, Pulipati VP. Dyslipidemia - Endocrine and Metabolic Disorders - MSD Manual Professional Edition [Internet]. 2021 [cited 2022 Aug 10]. Available from: https://www.msdmanuals.com/professional/endocrine-and-metabolic-disorders/lipid-disorders/dyslipidemia
41. Miao J, Zang X, Cui X, Zhang J. Autophagy, hyperlipidemia, and atherosclerosis. In: Advances in Experimental Medicine and Biology. Springer; 2020. p. 237–64.
42. Muller C, Salvayre R, Nègre-Salvayre A, Vindis C. HDLs inhibit endoplasmic reticulum stress and autophagic response induced by oxidized LDLs. Cell Death Differ. 2011;18(5):817–28.
43. Zhang Q, Zhang Q, Li Y, Liang T, Liang T, Lu X, et al. ER stress and autophagy dysfunction contribute to fatty liver in diabetic mice. Int J Biol Sci. 2015;11(5):559–68.
44. Perrotta I, Aquila S. The role of oxidative stress and autophagy in atherosclerosis. Oxid Med Cell Longev. 2015;2015.
45. Martinez-Useros J, Garcia-Foncillas J. Obesity and colorectal cancer: Molecular features of adipose tissue. Vol. 14, Journal of Translational Medicine. 2016. p. 21.
46. White CR, Datta G, Giordano S. High-Density Lipoprotein Regulation of Mitochondrial function. Adv Exp Med Biol. 2017 May 1;982:407.
47. Sebastián D, Palacín M, Zorzano A. Mitochondrial Dynamics: Coupling Mitochondrial Fitness with Healthy Aging. Vol. 23, Trends in Molecular Medicine. Elsevier Ltd; 2017. p. 201–15.

48. Youle RJ, Van Der Bliek AM. Mitochondrial fission, fusion, and stress. Vol. 337, Science. 2012. p. 1062–5.
49. Suárez-Rivero J, Villanueva-Paz M, de la Cruz-Ojeda P, de la Mata M, Cotán D, Oropesa-Ávila M, et al. Mitochondrial Dynamics in Mitochondrial Diseases. Diseases. 2016;5(1):1.
50. Forte M, Schirone L, Ameri P, Basso C, Catalucci D, Modica J, et al. The role of mitochondrial dynamics in cardiovascular diseases. Vol. 178, British Journal of Pharmacology. 2021. p. 2060–76.
51. Ott M, Gogvadze V, Orrenius S, Zhivotovsky B. Mitochondria, oxidative stress and cell death. Vol. 12, Apoptosis. 2007. p. 913–22.
52. Murphy MP. How mitochondria produce reactive oxygen species. Vol. 417, Biochemical Journal. 2009. p. 1–13.
53. Li X, Fang P, Li Y, Kuo YM, Andrews AJ, Nanayakkara G, et al. Mitochondrial reactive oxygen species mediate lysophosphatidylcholine-induced endothelial cell activation. Arterioscler Thromb Vasc Biol. 2016;36(6):1090–100.
54. Hulsmans M, Van Dooren E, Holvoet P. Mitochondrial reactive oxygen species and risk of atherosclerosis. Curr Atheroscler Rep. 2012;14(3):264–76.
55. Jebari-Benslaiman S, Galicia-García U, Larrea-Sebal A, Olaetxea JR, Alloza I, Vandenbroeck K, et al. Pathophysiology of Atherosclerosis. Vol. 23, International Journal of Molecular Sciences. Multidisciplinary Digital Publishing Institute; 2022. p. 3346.
56. Lamon BD, Hajjar DP. Inflammation at the molecular interface of atherogenesis: An Anthropological Journey. Vol. 173, American Journal of Pathology. 2008. p. 1253–64.
57. Roy P, Orecchioni M, Ley K. How the immune system shapes atherosclerosis: roles of innate and adaptive immunity. Vol. 22, Nature Reviews Immunology. Nat Rev Immunol; 2022. p. 251–65.
58. Gkikas I, Palikaras K, Tavernarakis N. The role of mitophagy in innate immunity. Front Immunol. 2018;9(JUN):1–15.
59. Chandel NS, Schumacker PT, Arch RH. Reactive Oxygen Species Are Downstream Products of TRAF-mediated Signal Transduction. J Biol Chem. 2001 Nov 16;276(46):42728–36.
60. West AP, Brodsky IE, Rahner C, Woo DK, Erdjument-Bromage H, Tempst P, et al. TLR signalling augments macrophage bactericidal activity through mitochondrial ROS. Nature. 2011;472(7344):476–80.
61. Lee MKS, Moore XL, Fu Y, Al-Sharea A, Dragoljevic D, Fernandez-Rojo MA, et al. High-density lipoprotein inhibits human M1 macrophage polarization through redistribution of caveolin-1. Br J Pharmacol. 2016;173(4):741–51.
62. Sanson M, Distel E, Fisher EA. HDL Induces the Expression of the M2 Macrophage Markers Arginase 1 and Fizz-1 in a STAT6-Dependent Process. PLoS One. 2013;8(8):6–13.
63. Smythies LE, Roger White C, Maheshwari A, Palgunachari MN, Anantharamaiah GM, Chaddha M, et al. Apolipoprotein A-I mimetic 4F alters the function of human monocyte-derived macrophages. Am J Physiol - Cell Physiol. 2010 Jun;298(6).

64. Sloop CH, Dory L, Roheim PS. Interstitial fluid lipoproteins. Vol. 28, Journal of Lipid Research. 1987. p. 225–37.
65. Mizushima N, Yoshimori T. How to interpret LC3 immunoblotting. Vol. 3, Autophagy. 2007. p. 542–5.
66. Kirkin V, McEwan DG, Novak I, Dikic I. A Role for Ubiquitin in Selective Autophagy. Vol. 34, Molecular Cell. 2009. p. 259–69.
67. Kim YC, Guan KL. MTOR: A pharmacologic target for autophagy regulation. Vol. 125, Journal of Clinical Investigation. American Society for Clinical Investigation; 2015. p. 25–32.
68. Mauvezin C, Neufeld TP. Bafilomycin A1 disrupts autophagic flux by inhibiting both V-ATPase-dependent acidification and Ca-P60A/SERCA-dependent autophagosome-lysosome fusion. Autophagy. 2015;11(8):1437–8.
69. Rovera G, Santoli D, Damsky C. Human promyelocytic leukemia cells in culture differentiate into macrophage-like cells when treated with a phorbol diester (12-0-tetradecanoylphorbol 13-acetate/adhesion/terminal differentiation/myeloid differentiation/monocytes). Vol. 76, Cell Biology. 1979.
70. Mineo C, Yuhanna IS, Quon MJ, Shaul PW. High density lipoprotein-induced endothelial nitric-oxide synthase activation is mediated by Akt and MAP kinases. J Biol Chem. 2003 Mar 14;278(11):9142–9.
71. Georgila K, Gounis M, Havaki S, Gorgoulis VG, Eliopoulos AG. mTORC1-dependent protein synthesis and autophagy uncouple in the regulation of Apolipoprotein A-I expression. Metabolism. 2020 Apr 1;105.
72. Murugesan G, Sa G, Fox PL. High-density lipoprotein stimulates endothelial cell movement by a mechanism distinct from basic fibroblast growth factor. Circ Res. 1994;74(6):1149–56.
73. Gerster R, Eloranta JJ, Hausmann M, Ruiz PA, Cosin-Roger J, Terhalle A, et al. Anti-inflammatory Function of High-Density Lipoproteins via Autophagy of IκB Kinase. CMGH. 2015 Mar 1;1(2):171-187.e1.
74. Wooten MW, Seibenhener ML, Mamidipudi V, Diaz-Meco MT, Barker PA, Moscat J. The Atypical Protein Kinase C-interacting Protein p62 Is a Scaffold for NF-κB Activation by Nerve Growth Factor. J Biol Chem. 2001 Mar 16;276(11):7709–12.
75. Lee YH, Ko J, Joung I, Kim JH, Shin J. Immediate early response of the p62 gene encoding a non-proteasomal multiubiquitin chain binding protein. FEBS Lett. 1998;438(3):297–300.
76. Benischke AS, Vasanth S, Miyai T, Katikireddy KR, White T, Chen Y, et al. Activation of mitophagy leads to decline in Mfn2 and loss of mitochondrial mass in Fuchs endothelial corneal dystrophy. Sci Rep. 2017;7(1).
77. Zhu S, Wang Y, Chen W, Li W, Wang A, Wong S, et al. High-density lipoprotein (HDL) counter-regulates serum amyloid A (SAA)-induced sPLA2-IIE and sPLA2-V expression in macrophages. PLoS One. 2016;11(11).

78. Tian H, Li Y, Kang P, Wang Z, Yue F, Jiao P, et al. Endoplasmic reticulum stress-dependent autophagy inhibits glycated high-density lipoprotein-induced macrophage apoptosis by inhibiting CHOP pathway. J Cell Mol Med. 2019;23(4):2954–69.
79. Rey-Giraud F, Hafner M, Ries CH. In vitro generation of monocyte-derived macrophages under serum-free conditions improves their tumor promoting functions. PLoS One. 2012;7(8).
80. Xu ZX, Yang YZ, Feng DM, Wang S, Tang YL, He F, et al. Oxidized high-density lipoprotein promotes maturation and migration of bone marrow derived dendritic cells from C57BL/6J mice. Chinese Med Sci J. 2008;23(4):224–9.
81. Gao F, Ren YJ, Shen XY, Bian YF, Xiao CS, Li H. Correlation between the high density lipoprotein and its subtypes in coronary heart disease. Cell Physiol Biochem. 2016;38(5):1906–14.

8 CURRICULUM VITAE